QATAR UNIVERSITY

Graduate Studies

College of Arts and Sciences

ASSOCIATION BETWEEN INSULIN RESISTANCE AND NITRIC OXIDE IN HUMAN RETINAL MICROVASCULAR ENDOTHELIAL CELLS *IN VITRO*

A Thesis in

Department of Health Sciences

By

Sumbul Bushra

© 2015 Sumbul Bushra

Submitted in Partial Fulfillment

of the Requirements

for the Degree of

Master of Science/Arts

June 2015

COMMITTEE

The thesis of **Sumbul Bushra** was reviewed and approved by the following:

We, the committee members listed below accept and approve the Thesis/Dissertation of the student named above. To the best of this committee's knowledge, the Thesis/Dissertation conforms to the requirements of Qatar University, and we endorse this Thesis/Dissertation for examination.

Name: Dr. Nasser Rizk

Signature _____ Date_____

Name: Dr. Ahmad Al-Malki

Signature _____ Date_____

Name: Dr. Ali Eid

Signature _____ Date_____

Name: Dr. Christophe Triggle

Signature _____ Date_____

ABSTRACT

Diabetic retinopathy (DR) a major consequence of diabetes is considered the leading cause of vision loss and blindness worldwide among working adults. Endothelial dysfunction expediting imbalance in vascular homeostasis, is one of the primary manifestation leading to the pathogenesis of DR. NO a major vasodilator involved in the regulation of vascular homeostasis is reported to be released by insulin dependent PI3K/ Akt signaling pathway. Endothelial dysfunction impairs ocular hemodynamics by reducing the bioavailability of NO and increasing the production of reactive oxygen species (ROS) and may be responsible for the pathogenesis of vascular dysfunction in retinopathy.

In the current study in order to examine the effect of insulin on NO production, HRECs cells were cultured and grown in high glucose (30mM) and normal (5mM) glucose for 24 hours. Subsequently, the cells were treated with 100nM insulin for 10 minutes, 1, 2, and 4 hours. The various parameters of PI3K/ Akt signaling pathway were analyzed.

This study demonstrated that Hyperglycemia causes an increase in ROS/oxidative stress and apoptosis, while insulin promotes a significant decrease in ROS and apoptosis, eNOS mediated NO production increases with hyperglycemia but remarkably reduced with insulin treatment after 1hour, 2 hours and 4 hours. This may suggest that insulin could counteract the hyperglycemic effect on AKT/PI3 kinase which mediates NO production and VEGF-A, with decreased adhesion molecules such as p-selectin that is involved in barrier disorder of retinal endothelial cells. In summary, insulin could counteract the deleterious effects of hyperglycemia on retinal endothelial cells via various molecular approach including oxidative stress, apoptosis, NO, and adhesion molecules.

TABLE OF CONTENTS

LIST OF FIGURES

LIST OF TABLES

LIST OF ABBREVIATIONS

Abbreviations	Explanation
Akt	Protein Kinase B
DR	Diabetic Retinopathy
eNOS	Endothelial Nitric Oxide Synthase
HRMECs	Human Retinal Microvascular Endothelial Cells
IRS-1	Insulin Receptor Substrate-1
IRS-2	Insulin Receptor Substrate-2
NO	Nitric Oxide
NFkB	nuclear factor kappa-light-chain-enhancer of activated B cells
PI3K	Phosphatidylinositol 3-Kinase
VEGFA	Vascular Endothelial Growth Factor- Angiogenesis

DECLARATION

I hereby declare that this thesis entitled **Association Between Insulin Resistance And Nitric Oxide In Human Retinal Microvascular Endothelial Cells *In Vitro*** is my own original work and has not been previously submitted for any degree in any other university.

I further declare that all the sources used or quoted in this thesis have been indicated and acknowledged.

Sumbul Bushra

ACKNOWLEDGMENT

Firstly and above all, I tribute all achievements to the **merciful mighty Allah**, the almighty, on whom we depend for sustenance and guidance. I extend my heart felt gratitude to all people that contributed for the fulfillment of this work.

My appreciation and gratitude for **Qatar University supervisor**, committee, and staff. I would like extend special thanks to my supervisor **Dr. Nasser Rizk** and his entire research team for all the support and guidance, with special gratitude for **Dr. Isha Sharma** for patiently guiding and teaching me all the new techniques and experiments. I would also extend my heart felt gratitude to my co-supervisors **Dr. Ahmed Malki** at **Department of Health Sciences** and **Dr. Ali Eid at Department of Biological and Environmental Sciences**. To the **Dr. Ali Eid's Cell Culture Lab** and **Mr. Alaa** at the Department of Biological and Environmental Sciences for generously allowing me to use the culture facility. A special thanks to the entire team of **Biomedical Research Center**. . A special thanks to my external examiner **Dr. Christophe Triggle** for all your questions and suggestion, they really opened new aspects to the project. I would like to extend my gratitude to the **Department of Health Sciences and Biomedical Science Master program**. All the graduate students and professors have been very supportive. I thank you for all your questions and feedback; it has made me better!

Last but not the least, I would like to thank **my parents and family** for their support and prayers, without them I would not have been able to do anything.

INTRODUCTION

Obesity and type 2 diabetes is characterized by insulin resistance which has been reported as the major risk factors associated with the development of the endothelial dysfunction and vascular complications such as atherosclerosis. Induction of the vascular dysfunction is obviously a proved metabolic consequence of insulin resistance.

Diabetes leads to altered retinal microvascular function and ultimately diabetic retinopathy. Insulin signaling may play a role in this process, and animal studies indicated a role of the insulin in the pathogenesis of retinal neovascularization through its effect on endothelial cells. Endothelial dysfunction impairs ocular hemodynamics by reducing the bioavailability of NO and increasing the production of reactive oxygen species (ROS) and may be responsible for the pathogenesis of vascular dysfunction in retinopathy. Nitric oxide (NO) well known to play a significant role in the cardiovascular systems functions is reported to be released through the insulin stimulated PI3K/Akt signaling pathway. Several factors are postulated to be associated with the reduced production of NO of the vascular endothelium in inulin–resistant states such as impairment of eNOS production, and PI3K activation.

Insulin resistance would impair the production of NO in retinal vascular endothelial cells. Until now, the pathophysiology of retinal vascular dysfunction due to high glucose load and insulin resistance in association with NO bioavailability in these cells remains unclear. This study was thus designed in the interest to elucidate the correlation between hyperglycemia and insulin resistance in human retinal microvascular endothelial cells.

HYPOTHESIS

In diabetic arteries, endothelial dysfunction seems to involve both insulin resistance specific to the Akt pathway and hyperglycemia. Hyperglycemia itself also inhibits production of nitric oxide in arterial endothelial cells. We hypothesize that hyperglycemia and insulin resistance would impair NO production in human retinal endothelial cells.

AIMS AND OBJECTIVES

The primary objective of this research is to elucidate the potential role of insulin and its signaling pathway on NO synthesis on the human retinal microvascular endothelial cells (HRECs) exposed to high glucose load to induce insulin resistance.

In order to achieve the general aim, the study had the following endpoints:

1) Assess the production of NO in the condition medium and the cell lysate
2) Assess the expression of endothelial NO synthase (eNOS)
3) Assess the insulin signaling pathway at the protein levels and phosphorylation of: IRS1.
4) Assess the expression of angiogenic, adhesion molecules and inflammatory markers : VEGFA, P-Selectin and NFkB.

CHAPTER 1

LITERATURE REVIEW

1.LITERATURE REVIEW:

1.1 Diabetes

Diabetes is characterized by the persistent increase in blood sugar levels (hyperglycemia). It occurs as a consequence of inadequate production of insulin, known as type 1 diabetes, or in association with obesity and metabolic syndrome, known as type 2 diabetes resulting from resistance to endogenous insulin (Favero, Paganelli, Buffoli, Rodella, & Rezzani, 2014). Impaired endothelial functions in diabetes could aid the reduction in insulin availability to the tissue; thus decreasing insulin sensitivity independently from its direct effector ions in the muscle cells (Kolka & Bergman, 2013). Endothelial impairment, in type I diabetes are preponderantly reported to be caused by metabolic changes mainly at retinal and kidney levels by hyperglycemia and microvascular complications (Giacco & Brownlee, 2010). Contrary to this in type 2 diabetes, the association between endothelial dysfunction and diabetes are depicted as more complex, due to the initiation of endothelial dysfunction well before the onset of diabetes(Caballero et al., 1999). Type 2 diabetes is characterized by insulin resistance that has been reported as the major risk factor associated with the development of endothelial dysfunction and vascular complications such as atherosclerosis.

1.2 Epidemiology

Diabetic retinopathy (DR) a major impediment of diabetes is considered the leading cause of vision loss and blindness worldwide among working adults. According to the World Health Organization (WHO)("World Health Organization," 2015), the global prevalence of diabetes in 2014 had been estimated to be 9% among adults aged 18 years and above. As updated in November 2014, diabetes has been foreseen to become the 7th leading cause of

death worldwide by the year 2030 ("World Health Organization," 2015). Presently of the 347 million people worldwide enduring diabetes, approximately10% have a severe visual impairment, and 2% become blind (World Health Organization , 2015). Reckoned as a multifactorial progressive retinal disease DR, abides an extremely complex pathogenesis involving many different cells, molecules, and factors. The dilapidating consequences of diabetes results in the impairment of major retinal cells including Muller, pigment epithelial, ganglion as well as endothelial cells (Cheung, Mitchell, & Wong, 2010).

1.3 The vascular endothelium

The vascular endothelium consists of a thin layer of cells lining the lumen of the blood vessels that plays a vital role in maintaining homeostatic processes. It bestows a physical barrier between the blood vessel wall and the lumen (Wheatcroft, Williams, Shah, & Kearney, 2003). Endothelium secretes a number of mediators that instigate the control of vascular tone, transacting blood and nutrients into and out of the blood stream, vascular permeability, vasculogenesis, and angiogenesis (Cines et al., 1998; Pries & Kuebler, 2006; D. Y. Yu, Yu, Cringle, Kang, & Su, 2014). Figure1.1 briefly illustrates the major function of the vascular endothelium.

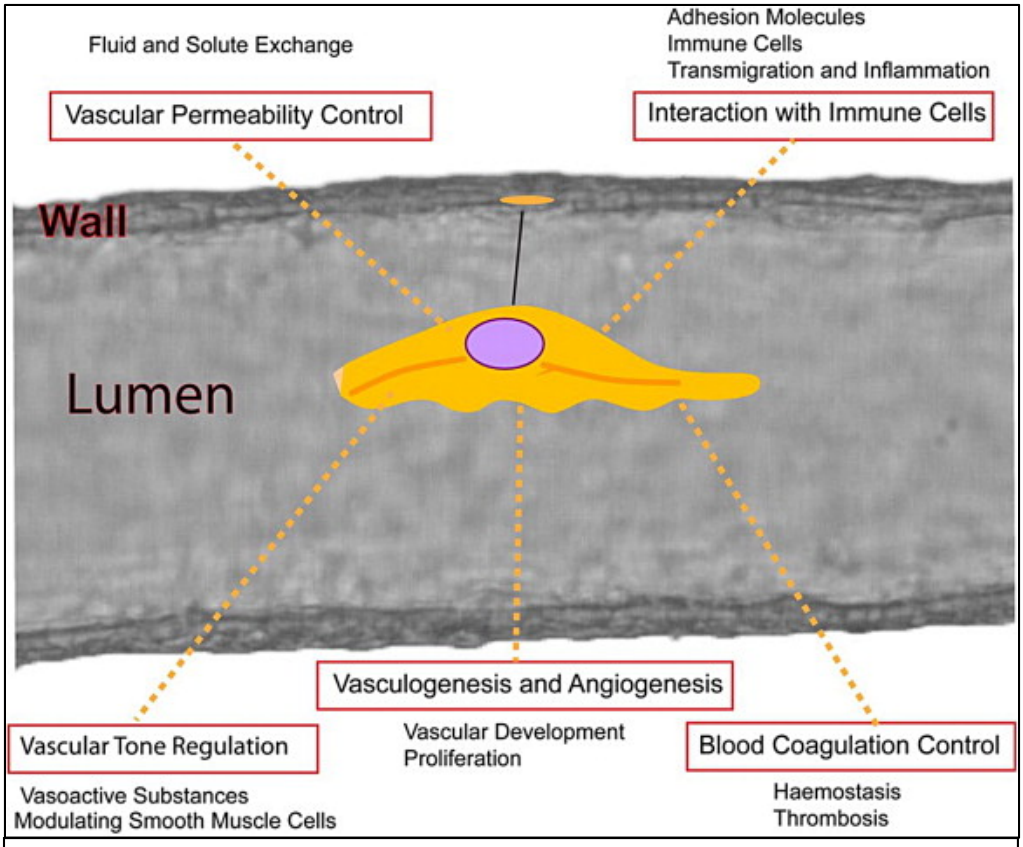

Figure1.1. Frame grabbed image of an isolated perfused porcine retinal artery. Five major functions are schematically illustrated. These functions collectively serve to regulate vascular supply to tissues. Endothelial dysfunction plays crucial roles in the pathology of vascular failure. (D. Y. Yu, Yu, Cringle, Kang, & Su, 2014)

Vascular tone is modulated by the production and release of various vasodilator and vasoconstrictor mediators. Endothelial derived vasodilators include nitric oxide (NO), prostacyclin (PGI_2) and endothelium-derived hyperpolarizing factor (EDHF); whereas vasoconstrictors include endothelin-1 and thromboxane A_2 (Wheatcroft, Williams, et al., 2003; D. Y. Yu et al., 2014). Retinal arterioles belong to the category of small resistance arterioles requiring an exquisite balance between vasodilator and constrictor influences. This balance is crucial in order to appropriately adjust to various factors such as shear stress, temperature changes and blood volume variations (D. Y. Yu et al., 2014).

Endothelial dysfunction is defined as a flawed release of endothelium-mediated vasodilators along with disarticulated endothelial adhesion molecules and chemokines expression. Oxidative stress, diabetes and insulin resistance are among the multitude of pathogenic stimuli that impel vascular endothelial dysfunction. In many systemic diseases and retinal diseases, oxidative stress is considered an important initial pathogenic step leading to retinal ischemic disease, diabetic retinopathy, inflammation and glaucoma (Bharadwaj et al., 2013).

1.4 Nitric oxide production in vascular endothelium

1.4.1 Nitric oxide synthases

Nitric oxide synthases (NOS) are three distinct set of isoforms that catalyzes the synthesis of nitric oxide from L-arginine. Products of three different genes located on chromosomes 7,17 and 12; NOS isoforms are endothelial (eNOS, or NOS III), neuronal (nNOS, or NOS I) and inducible NOS (iNOS, or NOS II) (Alderton, Cooper, & Knowles, 2001; Andrew & Mayer, 1999). Activation of nNOS and eNOS via the calcium/calmodulin complex leads to the production of nitric oxide (NO). However, contrary to this iNOS are generated in the presence of immunological and inflammatory stimuli (Schmetterer & Polak, 2001). The enzymatic activity of NOS requires oxygen, nicotinamide adenine dinucleotide phosphate (NADPH) and essential cofactors flavin mononucleotide (FMN), falvin adenine dinucleotide (FAD), haem and tetrahydrobiopterin (BH_4) for NO generation (Kearney et al., 2008).

1.4.2 eNOS

eNOS being the principal source of endothelial NO is of preeminent importance for the normal vascular system functioning. It is activated by both hormonal factors such as insulin (Kearney et al., 2008; Sobrevia, Nadal, Yudilevich, & Mann, 1996), vasopressin (Kearney et al., 2008; Resta, Gonzales, Dail, Sanders, & Walker, 1997), cytokines (Yoshizumi, Perrella, Burnett, & Lee, 1993) and mechanical forces such as sheer stress created due to blood flow through blood vessels (Dimmeler et al., 1999). In vitro studies reports indicated the induction of eNOS serine phosphorylation by shear stress, vascular endothelial growth factor (VEGF) and insulin through phosphatidylinositol-3 kinase (PI3K) pathway followed by downstream protein kinase Akt (Protein kinase B) phosphorylation. These in turn enhance NO synthesis without the use of calcium/calmodulin complex pathway (Dimmeler et al., 1999; Toda & Nakanishi-Toda, 2007).

1.4.3 Nitric Oxide production

eNOS stimulated NO production regulation is a complex process. eNOS is reported to be stimulated by two mechanisms either in a calcium dependent manner or in calcium independent manner. L-arginine when transformed through N^G-hydroxy-L-arginine to L-citrulline due to the catalysis of NOS in the presence of oxygen and cofactors leads to NO production (Toda & Nakanishi-Toda, 2007).

1.4.4 Insulin stimulated NO production

Earlier works demonstrate NO production in a cultured endothelial cell under the influence of wortmannin-sensitive stimulation leading to insulin directed vasodilation. Various studies have established that though eNOS is constitutively expressed; both shear

stress and insulin are reported to elevate endothelial NO production through the phosphorylation of PI3K and activated Akt leading to eNOS phosphorylation (Salt, Morrow, Brandie, Connell, & Petrie, 2003; Scherrer, Randin, Vollenweider, Vollenweider, & Nicod, 1994).

Independent *in vitro* studies conducted on bovine aortic endothelial cells (BAECs) (Kim, Gallis, & Corson, 2001; Montagnani, Chen, Barr, & Quon, 2001), human umbilical vein endothelial cells (HUVEC) (Zeng & Quon, 1996), and kidney collecting duct cells (Pandey et al., 2015) proposed rapid insulin-receptor substrate-1 (IRS-1) or IRS-2 tyrosine phosphorylation following insulin stimulation. This was followed by IRS-1 associated PI3K activation, in turn leading to phosphorylation and activation of Akt, Ser^{1177} specific site eNOS phosphorylation, and NO production. Figure1.2. Below illustrates insulin stimulated endothelial cell NO release and vasodilatation.

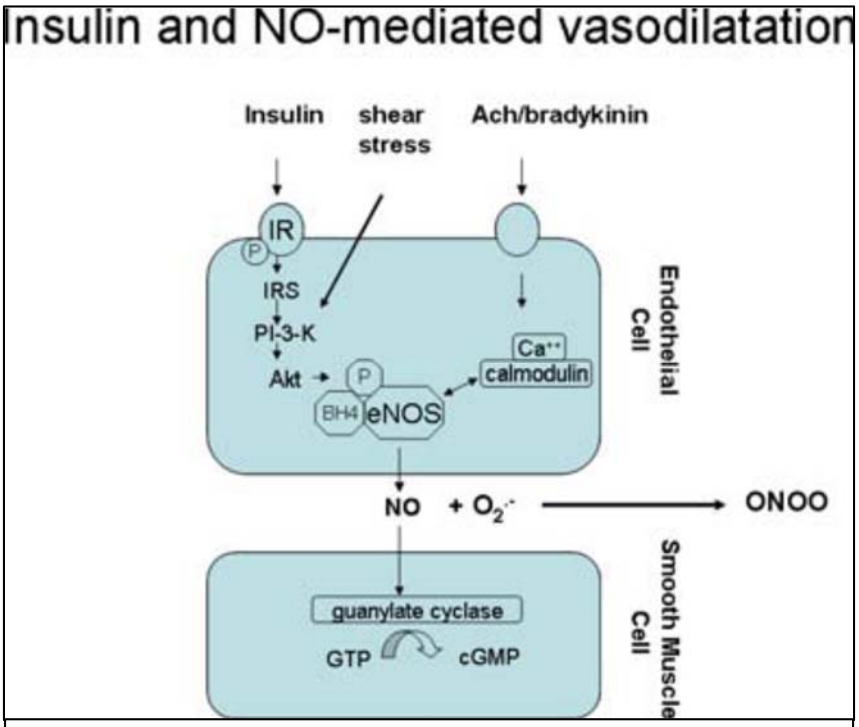

Figure 1.2.Insulin and endothelial cell NO release(Kearney, Duncan, Kahn, & Wheatcroft, 2008)

1.4.5 Other eNOS products

Compelling studies proclaim eNOS can directly or indirectly catalyze compilation of reactive oxygen species (ROS) within the vascular wall. These include nitroxyl (NO^-) ions, peroxynitrite ($ONOO^-$), superoxide (O_2^-) and nitrosothiols. Uncoupling of eNOS due to NADPH oxidation leads to increased vascular superoxide production (Griendling, Sorescu, & Ushio-Fukai, 2000). This process in turn decreases NO synthesis (Vásquez-Vivar et al., 1998). Another major mechanism of eNOS uncoupling is depicted by BH_4 depletion or oxidation and converting it to its inactive form dihydrobiopterin(BH_2), expediting superoxide production which decreases NO synthesis (Cosentino & Lüscher, 1998; Mortensen & Lykkesfeldt, 2014). Superoxide upon reaction with NO form peroxinitrite and nitrate. Peroxinitrite may activate redox signaling cascades inducing endothelial destruction or in turn may enhance O_2^- production and reduced NO synthesis through further oxidation and uncoupling of eNOS (Zou, Shi, & Cohen, 2002).

1.5 *Role of Nitric Oxide*

NO as free radical acts primarily in an autocrine or paracrine fashion, due to its extremely short half-life of only 3-6 seconds (Mayer & Hemmens, 1997). NO once produced, activates soluble enzyme guanylyl cyclase that catalyzes the formation of cyclic guanosine monophosphate (cGMP) from guanosine triphosphate. At physiological concentrations NO result in the phosphorylation of multitude of molecules involved in the smooth muscle relaxation. This leads to cGMP stimulated vasodilation of endothelial cells (Gewaltig & Kojda, 2002; Toda & Nakanishi-Toda, 2007). Apart from vasodilation, endothelial NO induces a reduction in vascular resistance, reduces blood pressure,

interrupt platelet aggregation and adhesion, leukocyte adhesion and transmigration, prohibits smooth muscle cell proliferation and prevent atherosclerosis (Förstermann, 2008, 2010).

1.6 *Insulin resistance and endothelial dysfunction*

Insulin resistance is defined as glucose-insulin homeostasis imbalance whereby, there is decreased glucose uptake in the peripheral tissues in response to insulin. Another factor closely related is hyperinsulinemia that occurs as a consequence of insulin resistance while both are risk factors for vascular disorders. Though insulin resistance is strongly associated with endothelial dysfunction yet, insulin resistance being the cause or result is disputed (Kearney et al., 2008; Wheatcroft, Williams, et al., 2003). An *in vivo* analysis of eNOS-knockout mice showed insulin resistance when compared to their wild-type counterparts. This indicates insulin resistance could be a maker in preference to the causative agent of endothelial dysfunction (Shankar, Wu, Shen, Zhu, & Baron, 2000). Clinical studies suggest insulin-resistant patients presenting increased circulating levels of endothelin-1 (ET-1), a potent vasoconstrictor. Vasodilators and vasoconstrictors balance is further aggravated due to the increased production of ET-1 following NO and ET-1 reciprocal activity. Studies have shown PI3K inhibition by ET-1 in smooth muscles exacerbating impaired vasodilation and endothelial dysfunction (Groop, Forsblom, & Thomas, 2005; Kalani, 2008). In a vivo study conducted on rats demonstrated ET-1 stimulating increased NADPH oxidase-dependent ROS generation, which led to attenuate NO bioavailability. This further lead to endothelial dysfunction and increased vasoconstriction (Sánchez et al., 2014).

1.7 *Insulin resistance and diabetic retinopathy*

Induction of the vascular dysfunction is actually a metabolic consequence of insulin resistance (Chakravarthy, Hayes, Stitt, McAuley, & Archer, 1998). Diabetes leads to altered retinal microvascular function and ultimately diabetic retinopathy. The evidently reported causative agents encompassed in the pathophysiology of DR include factors like glucose, insulin, advanced glycation end products(AGE), lipids and lipoproteins, growth factors and cytokines such as vascular endothelial growth factor (VEGF), insulin like growth factor (IGF), intracellular mediators such as phosphatidylinositol 3 kinase(PI3K), protein kinase C (PKC), vasoactive substances such as nitric oxide (NO); oxygen free radicals such as superoxide anion radical (O_2^-) and various other factors (Ahsan, 2015; Ola et al., 2012). Disruption in metabolites within diabetic retina alters the production pattern of a number of mediators including growth factors, neurotrophic factors, cytokines/chemokines, vasoactive agents, inflammatory molecules, coagulation factors, and adhesion molecules. These disruptions in turn prompt increased blood flow, increased capillary permeability, altered cell turnover (apoptosis), and finally angiogenesis (Ola et al., 2012). Multitudinous investigative compilations suggest that the increment in fluxes attained via these pathways may lead to a cascade of events resulting in the induction of retinal damage leading to DR. These include the promotion of apoptosis, inflammation and angiogenesis. (Ola et al., 2012)

During the early stages of the development of diabetes, intracellular hyperglycemia causes abnormalities in blood flow and elevated vascular permeability. As a consequence this leads to decreased function of vasodilators such as nitric oxide, increased activity of vasoconstrictors such as angiotensin II and endothelin-1. This causes an increase in the

permeability factors such as vascular endothelial growth factor (VEGF). Added up, these variations lead to edema, ischemia and hypoxia-induced neovascularization in the retina, proteinuria, mesangial matrix expansion and glomerulosclerosis in the kidney, and multifocal axonal degeneration in peripheral nerves (Figure1.3).

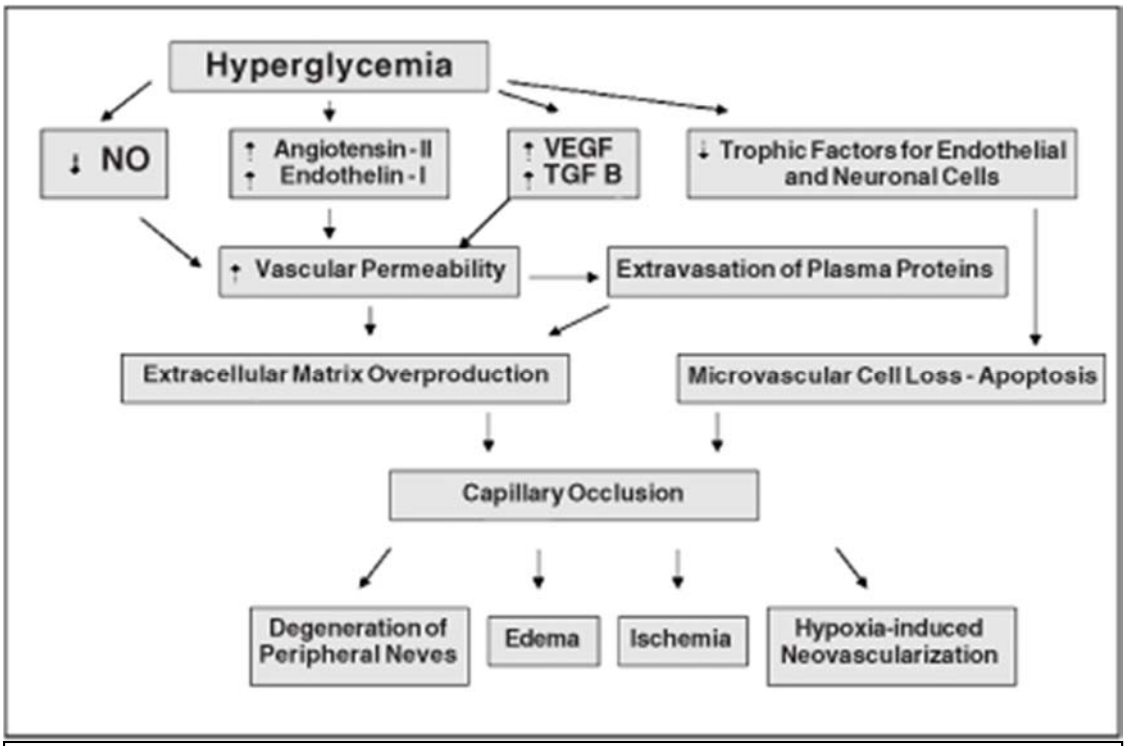

Figure1.3. Pathway to Consequences of Hyperglycemia (Alves, Carvalheira, Módulo, & Rocha, 2008).

1.8 *Endothelial dysfunction and Biochemical Changes:*

Among the several reported signs of DR micro aneurysm and hemorrhages are denoted as early signs, while dilated, tormenting, irregular and narrow retinal blood vessels known as retinal ischemia are later signs that ultimately result in neovascularization (Chen, Liu, Xiao, & Lu, 2014; Gao, Zhu, Tang, Wang, & Ren, 2008). Earlier studies have reported hyperglycemia to be a contributing factor in retinal capillary damage and modifications in retinal hemodynamics, ensuing in hypoxia state and elevated tissue production of

angiogenic factors in both early and later stages of diabetic retinopathy by activation and dysregulation of many metabolic pathways (Gao et al., 2008). High glucose concentrations within the cells could increase flux through the activation of various pathways such as glycolytic pathway, hexosamine pathways and stimulation of PKC and PI3K leading to increased ROS production, with the induction of oxidative stress, apoptosis, inflammatory response, and promotion of angiogenesis (Kowluru & Chan, 2007; Ola et al., 2012; Yamagishi & Matsui, 2011). Several conflicting studies suggest that hyperglycemia may not be an inducer or contributor to the range of cellular and functional changes in the pathophysiology of DR (Kowluru, Abbas, & Odenbach, 2004).

1.8.1 Insulin induction and VEGF expression

Numerous growth factors and cytokines have been entailed to play a role in the pathogenesis of retinal neovascular diseases. Previous studies account vascular endothelial growth factor (VEGF) to serve as a primary stimulator of capillary formation and enhanced cell permeability inducing the vascular pathology of diabetic retinopathy (Wu et al., 2010). Preclinical and clinical studies have evinced intraocular VEGF elevation in the eyes of diabetic patients with blood-retinal barrier breakdown and neovascularization following injury triggered by oxygen stress and hyperglycemia (Wheatcroft, Kearney, et al., 2003). Lately, the VEGF expression in numerous cell types such as fibroblast, epithelial cells and others have been stipulated to be increased in response to insulin; thereby amalgamated with the worsening of diabetic retinopathy following acute intensive insulin therapy (Zeng & Quon, 1996). The mode of VEGF expression though remain poorly understood has been reported to be regulated by numerous growth factors and cytokines, inclusive are interleukin 1-β, platelet-derived growth factor (PDGF) and transforming growth factor β.

(X. Du, Stocklauser-Färber, & Rösen, 1999). *In vitro* studies reportedly display insulin-induced VEGF expression at normal glucose levels (5mM) to be mediated through the activation of phosphatidylinositol 3-kinase/Akt (PI-3K), a downstream element of the insulin receptor. *In vitro* studies in bovine retinal microvascular endothelial cells (BRECs) and Human umbilical vein endothelial cells (HUVEC) at 30mM glucose concentration mimicking hyperglycemic state (Wu et al., 2010) along with Human retinal endothelial cells (HREC) at 15mM and 25mM glucose concentration have demonstrated an increase in VEGF expression(Gao et al., 2008).

1.8.2 Insulin resistance and proinflammatory mediators

Nuclear factor kappa B (NF-κB) is a nuclear transcription factor found in all cell types;(Patel & Santani, 2009) known to be activated in response to stress, hypoxia, viral proteins, bacteria and proinflammatory cytokines stimulus (Mitamura et al., 2003). NF-kB activation has been demonstrated to be either anti- or proapoptotic based on the cell type and disease state. Nonetheless, preclinical (Kowluru, Koppolu, Chakrabarti, & Chen, 2003) and clinical studies (Kowluru & Chan, 2007; Romeo, Liu, Asnaghi, Kern, & Lorenzi, 2002), have exhibited proapoptotic activity in the retina and its capillary cells in diabetes-induced NF-kB activation. *In vitro and in vivo* studies have shown that rat endothelial cells incubated with high glucose concentrations to have retinal NF-kB activation and elevation by approximately 60% (Kowluru et al., 2003). Gene expression levels of NF-kB in the epiretinal membranes in conditions such as proliferative diabetic retinopathy is reported to be significantly increased in a study performed by Mitamura et al. This result was confirmed by immunohistochemistry analysis (Mitamura et al., 2003). NF-kB activation is reported to transform the expression of multiple proinflammatory factors

conjointly tumor necrosis factor and inducible nitric oxide synthase; in turn resulting in an increment in free radical production (Griscavage, Wilk, & Ignarro, 1996; Kowluru et al., 2003). Kowluru et al. reported that high glucose following NF-kB activation lead to increase in oxidative stress and nitric oxide over 50% in the diabetic retinas of rats (Kowluru et al., 2003). However, the precise mechanism of NF-kB activation under hyperglycemia and insulin treatment consistent with diabetic retinopathy patient under treatment needs to be investigated.

1.8.3 Endothelial dysfunction and cellular adhesion molecules

Inflammatory cytokines are proclaimed to be upregulated in diabetic retinopathy with an evident increase in endothelial adhesion molecules such as ICAM1, VCAM1, PECAM-1 and P-selectin (Matsumoto et al., 2002; McLeod, Lefer, Merges, & Lutty, 1995; Rangasamy, McGuire, & Das, 2012). This is followed by the emancipation of inflammatory chemokines, cytokines and vascular permeability factors thereby leading to amended endothelial cell adherence and tight junction proteins (Kamiuchi et al., 2002). Consequently these distortions further impact the pathogenesis and progression of DR. ICAM1 (Intercellular Adhesion Molecule 1) also known as CD 54 encoded by ICAM1 gene are typically expressed on endothelial cells and immune system cells. ICAM1 though are continuously present in minimal concentration are reported to be upregulated upon cytokine stimulations. P-selectin also referred to as CD62P, the cell adhesion molecules though are expressed in megakaryocytes and endothelial; the expression levels are reported to be induced by inflammatory mediators (Ley et al., 1995; Rangasamy et al., 2012; Tedder, Steeber, Chen, & Engel, 1995). These adhesion molecules are proclaimed to play a focal portrayal in leukocyte adhesion to the endothelium amid inflammation and

pathogenesis of DR (Liu et al., 2005). Previous clinical comparative studies between normal, diabetic without retinopathy and DR patients evinced a significant increase in ICAM (Kamiuchi et al., 2002; Khalfaoui, Lizard, & Ouertani-Meddeb, 2008; McLeod et al., 1995; Penman et al., 2015).

Various independent studies have reported an elevated plasma P-selectin levels among DR patients in African Americans (Penman et al., 2015) and white subjects (Sobrin et al., 2011). The effect of the adhesion molecules ICAM1 and P-selectin at the level of retinal endothelial cells need to be elucidated for the better understanding of the DR pathogenesis under high glucose and insulin exposure though significant association has been found in cultured retinal glial cell at diabetic like high glucose concentration of 25mM(Melissa DeAnn Shelton, 2007).

1.8.4 Endothelial dysfunction and angiogenesis impairment

Two independent studies performed on HUVECs(P. Yu et al., 2006) and HREC(Chen et al., 2014) at 30mM glucose concentration demonstrated an increase in VEGF and PI3K-Akt pathway components at the mRNA levels assessed by reverse-transcription polymerase chain reaction(RT-PCR); furthermore the results were confirmed by protein expressions by western blot analysis. Cell migration through scratch wound assay investigated in both the studies at 5mM and 30mM medium glucose concentrations consistently evinced a significant decrease in the cell proliferation at a high glucose concentration in comparison to normoglycemia glucose concentrations. These studies denote high glucose as the rationale for alteration in PI3K and Akt signaling expediting into endothelial cell migration, proliferation and angiogenesis dysfunction.

1.8.5 Oxidative stress and apoptosis in endothelial dysfunction

Diabetes and hyperglycemia reportedly induce oxidative stress in the retina and may play a pivotal role in the development of DR by damaging retinal cells (Nakagawa et al., 2006). Approximately 0.1%-5% of oxygen under normal physiological conditions, are recorded to enter the electron transport chain eventually been reduced to superoxide; a reactive oxygen species (ROS). The remnants of the oxygen are imputed to be utilized in metabolic processes(Kowluru & Chan, 2007). Expanding documentations emphasize oxidative stress having critical involvement in the pathogenesis of diabetes and DR. Owing to the high energy demand and exposure to light retina are postulated to be particularly susceptible to oxidative stress(Kumari, Panda, Mangaraj, Mandal, & Mahapatra, 2008). In diabetic retina, the potential sources of reactive oxygen species (ROS) are still unclear, although a number of studies showed that interconnecting biochemical mechanisms endow to the pathogenesis of DR. Evident studies suggest that high glucose and the diabetic state vitalize flux via the glycolytic pathway, increase cytosolic NADH, increase tissue lactate to-pyruvate ratios. There is also an increased tricarboxylic acid cycle flux which may flood the mitochondria with electrons, thereby producing excess levels of ROS (Madsen-Bouterse & Kowluru, 2008). Other sources of ROS exemplified include inflammation, the polyol pathway and protein kinase C (PKC) activation stimulating mitochondrial overproduction of ROS(Brownlee, 2005). (Figure 1.4).

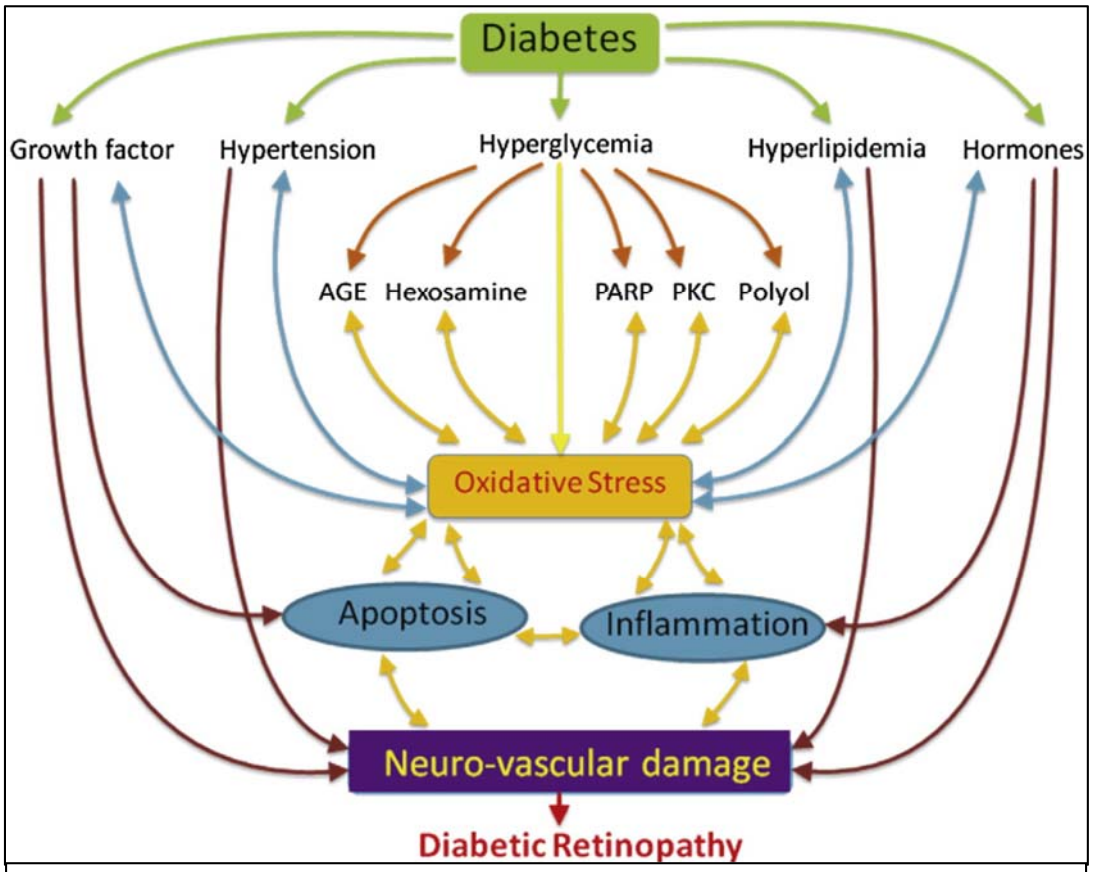

Figure1.4. General features for diabetes-induced neurovascular damage in DR. (Ola, Nawaz, Siddiquei, Al-Amro, & Abu El-Asrar, 2012)

Apart from the mitochondrial source of ROS other sources for the generation of ROS include cytochrome P450, the NADPH oxidases and nitric oxide synthases (Dröge, 2002). *In vivo* studies on streptozotocin induced diabetic rat showcased an increased production of ROS and similarly i*n vitro* studies on bovine retinal endothelial cells (BREC) incubated at 25mM glucose concentration significantly increased superoxide production in comparison to BREC cells incubated at 5mM glucose (Y. Du, Miller, & Kern, 2003).

Apoptosis of retinal capillary cells a consummated phenomenon is conventionally reported to be present in synchronization with oxidative stress. Sight-threatening unregulated angiogenesis and cell death are reported to be the progressive obliteration of DR (Mizutani, Kern, & Lorenzi, 1996). The molecular mechanism denoted for the induction of apoptosis

are reported to ROS-induced mitochondrial dysfunction eventually resulting in the activation of caspae-3 resulting in DNA fragmentation (Anuradha, Kanno, & Hirano, 2001; Phaneuf & Leeuwenburgh, 2002); diabetes induced proapoptotic NFkB activation (X. Du et al., 1999; Romeo et al., 2002). Exposure of rat retinal endothelial cells in an *in vitro* analysis at a glucose concentration of 25mM glucose medium endorsed a 50% increase in caspase-3 activity and hyperglycemia induced apoptosis, in comparison to cells exposed to 5mM glucose medium (Kowluru et al., 2004; Kowluru, Tang, & Kern, 2001). In vivo studies on alloxan diabetic rats for the duration of 2-14 months to have showed similar results with a significant elevation in apoptosis in comparison to control group(Kowluru & Koppolu, 2002). Du et al. reported in their study that long term exposure of human umbilical vascular endothelial cells(HUVEC) to 72 hours of high glucose concentration resulted in an increased generation of ROS, NFkB activation, Nitric oxide synthase dependent peroxynitrite formation and induction of apoptosis(X. Du et al., 1999). Independent studies have demonstrated a reduction in the hyperglycemia induced apoptosis upon treatment of endothelial cells with antioxidants and molecular inhibitors (Anuradha et al., 2001; Romeo et al., 2002).

CHAPTER 2

MATERIAL AND METHODS

2.1 Materials

Cryopreserved Human retinal microvascular endothelial cells (HREC) (ACBRI 181) purchased from Cell System; Complete Classic Medium Kit With Serum and Culture Boost (certificate No: 4Z0-500); Complete Serum-Free Medium Kit With Recombinant RocketFuel (Certificate No: SF-4Z0-500-R); (Certificate No: 4Z0-210) Attachment Factor (Certificate No: 4Z0-210); antibiotic: Bac-Off® (Certificate NO: 4Z0-643); Passage Reagent Group (Certificate No: 4Z0-800); PRG-2 Trypsin-EDTA Solution (Certificate NO: 4Z0-310); all were purchased from Cell System (Cell Systems, 12815 NE 124th Street, Suite A Kirkland, WA 98034)

Phosphate Buffered Saline (PBS) pH 7.4 (1X), was purchased from Gibco (Life Technologies, UK). TRIzol Reagent Ambion RNA [REF #15596026] was purchased from Life Technologies USA. Chloroform HPLC grade, Code: C/4966/15, was purchased from Fisher Scientific. RNase free water was from PreAnalytiX/ Qiagen, # 1057099 Hilden, Germany. Agilent RNA 6000 Pico Kit was from Agilent Technologies, Waldbronn- Germany. High Capacity RNA-to-cDNA kit was purchased from Applied Biosystems P/N 4387406. TaqMan Gene Expression Master Mix (P/N 4369016).

Tali™ image-based Cytometer from Invitrogen by Life Technologies (Catalog # T10796); CellROX® Oxidative Stress Reagents (Catalog # C10443); Tali™ Apoptosis Kit- Annexin V Alexa Fluor 488 & Propidium Iodide (Cat # A10788); Tali™ Cell Cycle Kit (Cat # A10798) ; Carboxy-H_2DCFDA , REF C400 (Cat # 1550062) were all purchased from Invitrogen by Life Technologies, USA.

BD Accuri™ C6 Flow Cytometer; Mouse Anti-HumanCD62E (Cat # 551145); PE Mouse Anti-Human CD54 (Cat # 555511) were all purchased from BD BioSciences, USA.

Pierce® RIPA Buffer (Cat# PF 201994); Pierce® BCA Protein Assay Kit (Cat# 23227) were all purchased from Thermo Scientific, USA.

Rb pAb Anti_IRS-1 (REF # AH01222), PI3K Total antibody (REF# 710400) wer purchased from Invitrogen. Rb Recombinant Oligoclonal Ab ladder- Broad range Marker (Sc-2361, Lot # G1013) from Santa Cruz Biotechnology. NuPAGE® Bis-Tris Mini Gela (Prod # IM- 8042) NOVEX® by Life Technologies, USA.

Ethical and Biosafety Approvals

Qatar University institutional review board has exempted this study, exemption number: QUST-CAS-SPR-13/14-20; see Appendix. Qatar university institutional Bio-safety committee has approved this study, approval number: QUST-CAS-SPR-13/14-20, see Appendix.

2.2 Methods

2.2.1 Human Retinal Microvascular Endothelial Cell culture

Cryopreserved HRMECs were rapidly thawed in a 37˚C water bath. Thereupon grown and passaged in tissue culture flasks wetted with attachment factor in CSC cell culture medium (CSC complete medium) with modified and optimized Dulbecco's Modified Eagle medium: nutrient mixture F-12(DMEM/F12) containing 10% fetal bovine serum (FBS), human recombinant growth factors (cultureBoost-R) a maintenance formulation to bring about quiescence to the cell culture for experimentation, 5mM normal human blood glucose concentration and Bac-off tonic (1:500 v/v dilution) containing synthetic fluoroquinone Ciprofloxacin for antibiotic treatment. No additional antibiotic was added to the medium. HRMECs were incubated at 37˚C with 5% CO_2 and used between passages 4 and 6 to minimize variability. Prior to experimentation HRMECs were seeded on the appropriate dish based on the assay either 100 mm, 6 well plates and 96 well plates. The culture media was changed at 24 hours followed by every 48 hours thereafter. Upon 80-90% confluency, HRMECs were serum starved for 6 hours by removing the growth medium and replacing it with CSC serum–free medium containing 0% FBS, containing 20% v/v human recombinant growth factors (Recombinant Rocket Fuel). Following starvation, prior to use the cells were maintained in CSC completed medium containing 5 or 25mM D-glucose to represent normal glucose control (NG, 5mM) and high glucose levels (HG, 30mM) for 24 hours. As per necessity osmotic control were used (Mannitol, 25mM). All the experiments were performed with 2 biological and total of 6 technical replicates.

Prior to subculture/culture manual cell count was performed routinely. Harvested cell resuspended in culture media were mixed in equal volume of staining dye Trypan Blue. 25µl cell suspension resuspended in 25µl of Trypan Blue were loaded on to hemocytometer (Bright Line) and counted under microscope. The numbers of cells counted in the middle 25 squares were used in the below formula to retrieve the total no of cells:

$$\frac{Total\ no.of\ Cells\ counted}{4(no.of\ squres)} \times 2(Dilution\ Factor) \times 10{,}000$$

Example: 1166/4 x 2x 10,000 = 5.8 x10^6 cells/ml

2.2.2 HRMECs Treatments

Prior to use for experimental analysis the culture plates were amassed into the following groups A and B with further subgrouping in A,A1, and B,B1. The group A1 and B1 were further sub grouped and incubated with 100nM insulin (Actrapid) for varying time points of 10 minutes, 1 hour, 2 hours and 4 hours.

Group A consisted of NG/control (5mM glucose), A1 (5mM glucose + 100nM Insulin for 10 minutes), A2 (5mM glucose + 100nM Insulin for 1 hours), A3 (5mM glucose + 100nM Insulin for 2 hours) and A4 (5mM glucose + 100nM Insulin for 4 hours). Group B consisted of HG/hyperglycemia (30mM glucose), B1 (30mM glucose + 100nM Insulin for 10 minutes), B2 (30mM glucose + 100nM Insulin for 1 hour), B3 (30mM glucose + 100nM Insulin for 2 hours) and B4 (30mM glucose + 100nM Insulin for 4 hours) . Figure 2.1 demonstrates the work plan for insulin treatment.

Actrapid is a fast or short-acting insulin with action onset within half hour and maximum effect approaching within 1.5-3.5 hours. The complete duration of action

for Actrapid insulin is approximately 7-8 hours. Based on the effectivity of the Actrapid insulin, various time points were chosen to analyze various types of parameters. Depending on the parameter to be analyzed the treated cell were harvested at the end of the treatment time points.

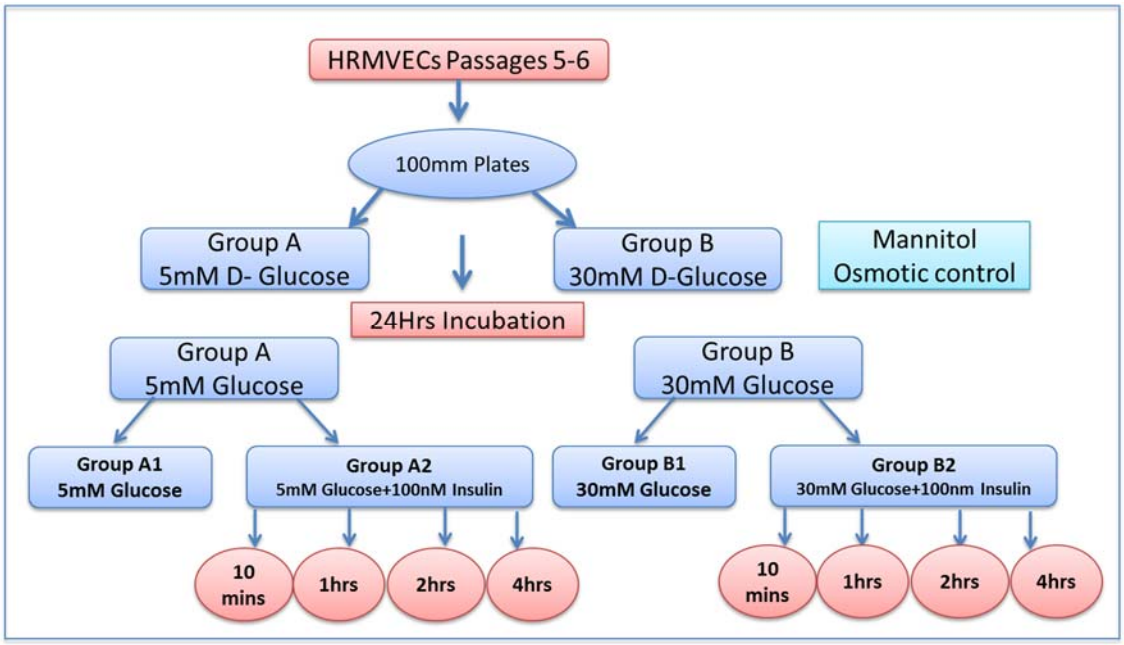

Figure 2.1. Insulin Treatment work plan (Prepared using Microsoft Word document)

2.2.3 Cell Growth Parameters

2.2.3(A) Cell Viability

The morphological cell size and count for each biological replicate was assessed prior to experimental procedures using Tali® Image-Based Cytometer. 25 µl of harvested cells washed, resuspended in 1X PBS were loaded into Tali Cellular Analysis slides. The average cell size and total cell concentrations for each sample were recorded.

The proportions of live and dead cells were assessed using Tali Dead Cell Red reagent, a ready-to-use solution containing propidium iodide (PI). PI is a fluorogenic DNA-binding dye used to identify necrotic cells. PI though impermeant to live cells,

gives red fluorescence upon binding to nucleic acids of the dead cell giving an enhanced fluorescence of 20 to 30 folds.

The treated cells were harvested by trypsinization using 3ml of 0.25% (v/v) Trypsin EDTA (TE), incubation at 37˚C for 5-7 minutes followed by centrifugation at 500x g and washing with PBS (phosphate Buffered Saline) prior to staining. 1 µl of Tali Dead Cell Red reagent was added to 100 µl sample cell suspension in microcentrifuge tube. The mixture was vortexed briefly and incubated in dark at room temperature for 1-5 minutes. 25 µl of the stained cells were loaded into Tali Cellular Analysis slide and cell viability of all samples were analyzed using Tali® Image-Based Cytometer at 535/617 nm excitation/emission (Ex/Em) wavelength.

2.2.3(B) Apoptosis

Apoptosis a carefully regulated cell death proceeding of normal cell development, if unregulated implicate disease state. The percentage apoptotic cells at discrete treatments were assessed using Tali Apoptosis Kit- Annexin V Alexa Fluor® 488 and Propidium Iodide. Annexin V has high affinity for phosphatidyl serine (PS), a characteristic of apoptotic cells where PS is translocated and exposed to the external cellular environment. PI as explained above binds to nucleic acids of dead cells.

Trypsinization using 3ml TE harvested the treated, incubation at 37˚C for 5-7 minutes followed by centrifugation at 500x g and supernatant was discarded. The cells were resuspended in 100 µl of 1X Annexin binding buffer (ABB) and 5 µl of Annexin V Alexa Fluor® 488 in a microcentrifuge tube. The mixture was vortexed briefly and incubated in dark at room temperature for 20 minutes. This was followed

by centrifugation at 500x g and resuspension in 100 µL of ABB and 1 µL of Tali® PI, brief mixing and incubation in dark at room temperature for 1-5 minutes. 25 µl of the stained cells were loaded into Tali® Cellular Analysis slide and percentage apoptosis of all samples were analyzed using Tali® Image-Based Cytometer at 488/499 nm and 535/617 nm Ex/Em wavelength for Annexin V Alexa Fluor® 488 and PI respectively.

2.2.3(C) Oxidative Stress

Cell-ROX® Oxidative Stress Reagents, fluorogenic probes were used to reliably measure ROS in live cells of all the various treatments. In the normally reduced cell states the cell-permeable reagents are reported to be non-fluorescent or weekly fluorescent while, exhibit strong fluorogenic signals at oxidation states.

Treated cells harvested using 3ml TE were centrifuged and resuspended in 200 µl PBS. 5µM (0.4 µl) Cell-ROX® orange reagent was added and the mixture was briefly vortexed followed by incubation at 37℃ for 30 minutes. This was superseded by centrifugation at 500x g, medium removal and cell wash three times with PBS. 25 µl of the stained cells were loaded into Tali Cellular Analysis slide and cell viability of all samples were analyzed using Tali® Image-Based Cytometer at 545/565 nm Ex/Em wavelength.

2.2.3(D) Cell Cycle Analysis

The amount of DNA in cells are precise reflection of the cell cycle phase therefore, cellular DNA content quantification for monitoring cell cycle progression of the treated HRMECs were performed using Tali® Cell Cycle Kit. Treated cells

trypsinized in 3ml TE, incubated at 37℃ for 5-7 minutes were harvested and resuspended in 200 µl PBS. This followed centrifugation at 500x g for 5minutes. The supernatant was removed and pellet resuspended in 200 µl PBS followed by second centrifugation for 5 minutes and transfer of tubes to ice. The PBS supernatant was discarded and cell pellet fixed slowly with 70% ice cold ethanol. The fixed samples were stored at -20˚C overnight prior to staining and analysis. Before staining the cells were centrifuged at 1000x g for 5minutes at 4˚ C, resuspended in 1ml PBS and recentrifuged at 500x g for 10 minutes at 4˚C. The washed cell pellet were incubated in 200 µl of Tali® Cell Cycle solution (all-in-one solution: PI, RNase A, and Triton® X-100) for 30 minutes in dark. Henceforth, the cells were briefly vortexed and 25 µl of the stained cells were loaded into Tali Cellular Analysis slide and cell viability of all samples were analyzed using Tali® Image-Based Cytometer at 535/617 nm Ex/Em wavelength.

2.2.4 Immunocytochemistry/ Fluorescent Microscopy

2.2.4(A) Reactive Oxygen Species (ROS)

6-carboxy-2',7'-dichlorodihydrofluorescein diacetate (Carboxy-H2DCFDA), a chemically reduced acetylated form of fluorescein was used as an indicator of ROS in live cells using fluorescent microscope. It is non-fluorescent molecules that upon reaction with intracellular esterase and oxidation by ROS readily are converted into green-fluorescent (BRANDT & KESTON, 1965).

Cells seeded in 6 well plates after treatments as mentioned in the above sections 2.2.1(A) and 2.2.1(B) were washed with PBS after the aspiration of culture media. The cells were incubated in 2ml prewarmed PBS and 10µM (2µl) Carboxy-H2DCFDA dye for 5-60 minutes at 37˚ C. The buffer was then replaced with prewarmed growth medium and multiple fluorescent images were captured using Immunofluorescent inverted microscope(Olympus X53) at~ 492-495/517-527 nm Ex/Em wavelength.

2.2.4(B) Reactive Nitrogen Species (RNS)

Intracellular NO was analyzed with DAF-FM diacetate, a cell-permeant nonfluorescent compound that passively diffuses across the cellular membrane and react with intracellular NO forming fluorescent benzotriazole (Kojima et al., 1998).

HRMECs seeded on 6 well plates after treatment as mentioned in the above sections 2.2.1(A) and 2.2.1(B). Adherent cells were incubated with 10µM (4µl) DAF-FM diacetate in 2 ml of culture media for 20-60 minutes at 4-37˚ C. Excess probes on cells were washed with PBS thereafter and incubated for additional 15-30 minutes in 2ml PBS to allow complete de-esterification of intracellular diacetates. At the fluorescence Ex/Em maxima of 495/515 nm the adherent cells were imaged for intracellular RNS concentration using Immunofluorescent inverted microscope (Olympus X53).

2.2.4(C) Fluorometric Nitric Oxide Assay

NO production was assessed using Abcam's Nitric Oxide Assay Kit (Fluorometric Cat # ab65327) indirectly by evaluating the level of its oxidized forms (nitrites and

nitrates) in all HRMECs seeded on 6 well plates after treatment as mentioned in the above sections 2.2.1(A) and 2.2.1(B). A standard curve was accomplished for the measurement levels between 0 and 1000 pmol/well standard. The cell lysate for all the treated samples were generated using the kit provided assay buffer. 75 µl of standards and samples in 96 well plates were exposed to 5 µl of enzyme cofactor and 5 µl of nitrate reductase with incubation at room temperature for 4 hours. Henceforth, 5 µl enhancer was added with 30 minutes incubation to quench interfering compounds. 5 µl of fluorescent DAN probe (2, 3 diaminonaphthalene) with 10 minutes incubation followed the addition of 5 µl NaOH with 10 minutes at room temperature incubation to enhance the fluorescent yield. The plates were read in fluorometer using Ex/Em= 360/450.

2.2.5 Cell Migration Assay

The effect of insulin on normal and high glucose induced migration of HRMEC was evaluated by scratch wound assay. In brief, upon 80-90% confluency of HRMECs in 6-well plates, the cells were starved with serum-free medium for 6 hours followed by 24 hours glucose treatment as described in sections 2.2.1(A) and 2.2.1(B). When the HRMECs had grown to confluence, a wound was made of appropriate width using 1000 µl pipette tip. Then, the HRMECs were washed with sterile 1xPBS to remove the floating cell. This was followed by incubation with complete medium containing 5mM and 30mM glucose concentrations and with or without 100nM insulin. The 6-well culture plates were incubated at 37 °C in a 5% CO2 incubator. The migration of cell monolayer was photographed (Olympus X53) at 0 hour, 2hrs, 4hrs and10hrs. Three fields were photographed for each well. The migration distance was measured

by using Microsoft Office Picture Manager. The experiment was performed with two biological replicates with similar results.

2.2.7 Gene Expression Analysis

2.2.7(A) RNA Extraction

Total RNA was extracted using an establish technique in the lab.

Briefly, treated cells as described in sections 2.2.1(A) and 2.2.1(B) were harvested with insulin treatment for 10mins and 1hrs in **TRIZOL**® reagent. 0.2 ml of chloroform was added to microcentrifuge tubes containing TRIZOL® homogenized samples shook vigorously. The time of 10min and 1hrs gene expression analysis where chosen since the gene expression/ transcription completes within 1 hour time span. The samples were centrifuged at 12,000 x g for 15 minutes at 4˚C and the aqueous layer was carefully recovered in fresh tubes. 0.5 ml of chilled 100% isopropanol was added to the aqueous layer. After incubation period of 10 minutes, the samples were centrifuged at 12,000 x g for 15 minutes. The pellet was washed with 1000 µl of 75% ethanol; air dried, resuspended in RNase-free water and quantified spectrophotometrically using Nano Drop. (A260/A280) and its quality was checked by the Agilent Bioanalyzer.

2.2.7(B) cDNA Preparation

To generate cDNA, 1000ng of total RNA was utilized with High Capacity RNA-to-cDNA Kit. The reaction mixture consisted of the following components per reaction for a total reaction volume of 20 µl: 10 µl 2X RT Buffer, 1.0 µl 20X Enzyme Mix, up to 9 µl RNA samples and quantity sufficient to 20 µl Nuclease-free water. Reverse

transcription reaction was performed in Thermo cycler (Gene Amp®, PCR System 9700).

2.2.7(C) Quantitative Real Time PCR

Quantitative Real time RT-PCR was performed using Applied Biosystem® 7500 Real Time PCR system and TaqMan® Gene Expression Master Mix (Applied Biosystem). The reaction mixture (total volume 10µl) consisted of the components as indicated in Table2.1. All the samples were quantified for IRS1, IRS2, eNOS, PI3K, Akt, NFkB and VEGFA. The primers are shown in Table2.2. Normalization was performed to Ubiquitin (UBC) to elucidate for differences in reverse transcription efficiencies of cDNA.

Table 2.1: RT-PCR Reaction Mixture

RT-PCR Reaction Mixture for IRS1, IRS2, eNOS, PI3K, Akt and NFkB	
Components	**Component Volume/Reaction (µl)**
20X PP (Primer)	0.5 µl
2X Master Mix	5 µl
cDNA	4 µl
Nuclease-free Water	0.5 µl
RT-PCR Reaction Mixture for VEGFA	
10X PP (Primer)	1 µl
2X Master Mix	5 µl
cDNA	4 µl
Nuclease-free Water	0 µl
RT-PCR Reaction Mixture for UBC	

40X PP (Primer)	0.25 µl
2X Master Mix	5 µl
cDNA	4 µl
Nuclease-free Water	0.75 µl

Table 2.2: Oligonucleotide sequences RT-PCR

Genes	Primer Sequences (5' ⟶ 3')
UBC (Human)	**IDT (Hs.PT.39a.22214853)**
IRS1 (Human)	**Life Technologies (Hs00178563_m1)**
IRS2 (Human)	**Life Technologies (Hs00275843_s1)**
eNOS (Human)	**Life Technologies (Hs01574659_m1)**
PI3K (Human)	**IDT (Hs.PT.58.96974)**
Akt (Human)	**IDT (Hs.PT.58.26215470)**
VEGFA (Human)	**IDT (Hs.PT.56a.1149801.g)**
NFkB (Human)	**IDT (Hs.PT.58.21008943)**

2.2.8 Protein Adhesion Assay by Flow Cytometer

Cell surface expression of adhesion molecules P-Selectin and ICAM1 on the control and treated cells were detected using BD Accuri ™ C6 Flow Cytometer (BD Biosciences). Cell-suspensions of pooled two biological replicates of the treated samples mentioned in the above sections 2.2.1(A) and 2.2.1(B) were stained with PE Mouse Anti-Human CD62E (P-Selectin) and PE Mouse Anti-Human CD54 (ICAM-1). 500 µl cell suspensions of all samples in 1XPBS were incubated in dark with 20 µl of the CD62E and CD54 antibodies respectively for 20 minutes. The cells were washed twice in 1XPBS prior to analysis by BD Accuri ™ C6 Flow Cytometer.

Unstained control cell suspensions in 1XPBS were used to create the gating based on the cell size and granularity by forward and side scatter. Analysis of 20,000 events was performed on BD Accuri ™ C6 Flow Cytometer using BD Accuri ™ C6 Analysis software.

2.2.9 VEGFA antibody analysis by ELISA

VEGFA antibody was detected in the condition medias of all samples using BioVendor Human VEGFA ELISA kit (Cat. No: RAF136R).

50 µL of the 1:2 dilute sample condition media and standard was added to the antibody coated micro-wells followed by incubation for 2 hours on a microplate shaker. Following the incubation unbound biological compounds were removed by washing followed by incubation with 100µL biotin conjugate for 1hr on microplate shaker. Unbound biotin-conjugated anti-Human VEGFA antibody was removed by washing. The samples were incubated with 100µL Streptavidin-HRP on the shaker for 1hrs to bin to the biotin-conjugated anti-Human VEGFA antibody. Following the washing step 100µL of TMB-substrate solution was added with incubation for 10 minutes leading to the formation of colored complex . 100µL of stop solution was added to terminate the reaction followed by absorbance reading at 620nm in TECAN® ELISA reader. The concentrations of the samples were calculated by plotting the absorbance Vs standard concentration curve.

2.2.10 Western Blotting

2.2.10(A) Protein Extraction

Confluent treated cultures as mentioned in the above sections 2.2.1(A) and 2.2.1(B) were washed twice with cold PBS to remove any traces of media. The cells were

homogenized using Thermo Scientific™ RIPA lysis and Extraction buffer, kept on ice for 5 minutes and collected using cell scraper. The collected lysate were centrifuged in a microcentrifuge tube at 14,000 rpm for 15 minutes at 4˚C. The supernatant was separated and stored in -80˚C until used for further analysis.

2.2.10(B) Protein Analysis

Protein analysis was performed using Pierce™ BCA Protein Assay Kit. Nine different BSA protein standards from 0-2000µg/mL were prepared. To perform the assay, 25µl of each BSA standards and test samples were pipetted in duplicate into a 96-well flat bottom ELISA plate followed by addition of 200µl of BCA working reagent. The samples were allowed to mix on a shaker followed by incubation at 37˚ C for 30 minutes. The samples were read spectrophotometrically at 562nm using TECAN Sunrise™ microplate reader. A 1:2 0r 1:3 dilution of samples were prepared if the samples were highly concentrated.

2.2.10(C) SDS-PAGE/Electrophoresis

SDS-PAGE was performed using ready to use NuPAGE® Bis-Tris Mini Gels. The gel plates after the removal of the gel cast comb were gently placed in to rigs and filled with 1X running buffer initially to check for leakage. The gaps between glass plates in the gel rig were then filled with 1X running buffer to immerse the gels completely in buffer. 40 µg of protein samples were at 95˚C for 5 minutes in 7.9 µl of loading buffer with 2% β-Merceptoethanol (βME), cooled on ice for 2 minutes followed by centrifugation at 5000 rpm for 1 minute. Equal amounts of proteins per sample were loaded each well of NuPAGE® Bis-Tris Mini Gels following the addition of molecular weight marker in the first well. The electrophoresis was run at

200 volts for 40-45 minutes. Upon the reaching of the dye from the loading buffer to the bottom of the gel, electrophoresis was terminated and plates removed. The stacking gel was cut and gel was removed from the cassette.

2.2.10(D) Western Blotting Protocol

The Bio-Rad semi-dry electroblot apparatus was prepared by placing 2 sheets of blotting pads, cut to the size of the gel and soaked in transfer buffer, on a ceramic transfer platform. One sheet of filter paper of exact the gel size soaked in transfer buffer was added next followed by the resolving gel. Next one sheet of nitrocellulose membrane exact size of the gel wetted in methanol was placed followed by one filter paper and two further sheets of blotting pads (all soaked in transfer buffer) (Figure 2.2). The lid was placed and was tightly secured close and the blot module was filled with transfer buffer until the gel/membrane sandwich gets covered in transfer buffer. The electroblot was run at a current of 30 volts for 1 hour.

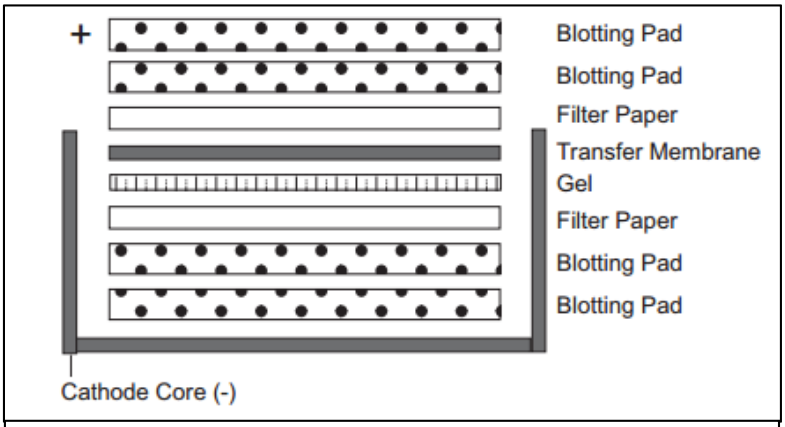

Figure 2.2: Western Blot Transfer Technique ("Life Technologies," 2015)

After transfer, the membrane was briefly rinsed in distilled water and the transfer efficiency was evaluated using Ponceau S Solution (Sigma Aldrich). The membrane

was rinsed again for 5-10 minutes to wash off Ponceau S dye. Blocking solution containing 5% (w/v) non-fat milk in 1X TBST (Tris Buffered Saline with Tween® 20) was used to incubate the membrane for one hour. After, incubation, it was incubated 1% (w/v) non-fat milk blocking solution containing 1:1000 dilution of the primary antibodies for the proteins of interest (Rabbit polyclonal Anti-IRS-1,Human PI3K Recombinant Rabbit Oligoclonal Antibody and Human Anti-Actin antibody) . The incubation was performed for overnight at 4˚C on the shaker.

Succeeding incubation, antibody containing blocking solution was removed and stored at 4˚C for future use. The membrane was rinsed 3 times with 1X TBST for 5-10 minutes and was reincubated in blocking solution containing 1:1000 dilution of secondary antibody for 3 hours at room temperature on a shaker. The secondary antibody used was species specific IgG conjugated anti-rabbit antibody. Post incubation, diluted antibody was removed and stored at 4˚ C for reuse. The membrane was rinsed 3 times in 1x TBST for 5-10 minutes. Immune complexes were detected using Western Blot Chemiluminescent Substrate ECL reagent containing substrates for horseradish peroxidase (HRP) or other probes. The membrane was incubated for 5 minutes in a HRP working solution consisting of equal volumes of stable peroxide solution (ECL A) and an enhanced luminal solution (ECL B). The chemical reaction with the antibodies and chemiluminescent substrate emits light at 425 nm captured with digital imaging device. Ten subsequent images were collected for each blot.

2.2.11 Statistical Analysis

Data were checked for normal distribution and are presented as mean (SD) for continues variables unless mentioned otherwise. Each experiment was independently repeated at least 3-5 times. All values in the figures are expressed as mean with standard deviation.

To determine statistical significance, the values were compared versus control and HG (as a control or reference day) with paired Student's t -tests. Statistical significance of difference between groups was tested using Student's t-test or if there were more than two groups, using one way analysis of variance (ANOVA) followed by posthoc analysis. A P value of .05 or less was considered to be significant. All calculations were performed using Graphpad prism 6 for windows.

CHAPTER 3

RESULTS

3. RESULTS

3.1 HRMECs Morphology and cell count

To study the effect of experimental hyperglycemia on insulin-stimulated HRMECs, the cells were carefully monitored for growth, morphology, vitality and their response to different treatments.

Cryopreserved HRMECs were resurrected and proliferated. The following Figure 3.1 was captured by an inverted microscope at 10x lens (Image A-E) which shows the procedural growth and proliferation in 100mm culture plates:

Image A. Day 0 Cell Seeding/Inoculation

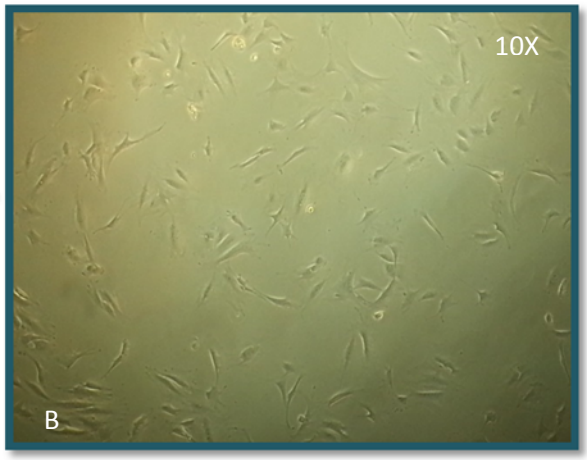

Image B. 24 hrs/Day2 after Inoculation- 10% Confluence

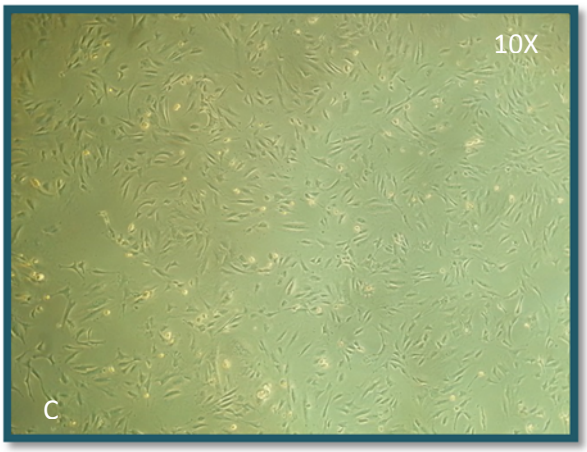

Image C. 96hrs/ Day 4 after Inoculation- 80-90% Confluence

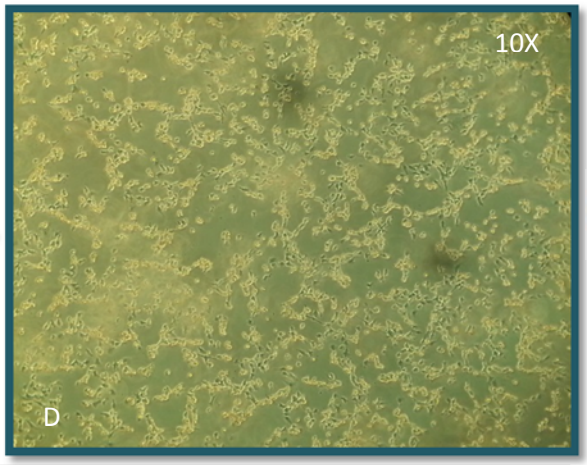

Image D. 6hrs of Serum Free Media treatment (Day 5)

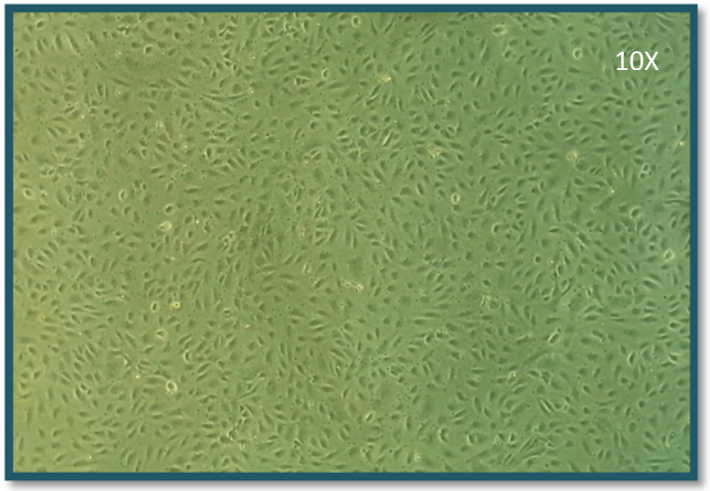

Image E. 24hrs after glucose treatment prior to Insulin treatments (Day 6)

Figure 3.1. HRMECs growth pattern. A, Day 0: seeded cells non-adherent to the culture plate. B, Day 2: cells adherent to the culture plate with 10% confluency. C, Day 4: 80-90% confluent cells necessary prior to different glucose treatments. D, Day 5: 6 hours Serum Free media treatment followed by 5 & 30mM glucose treatment. E, Day 6: 24 hours after glucose treatments followed by 100nM insulin treatment.

3.2 Cell Growth Parameters

3.2.1 Cell Viability

The viability of the cell is an important parameter performed to assess the viability, uniformity and standardization of all type of cell samples used in the experimental procedure. These are imperative in verifying the health of the cells in culture as well as the extent of toxicity of the treatments during experimental propagation. The morphological assessment was performed by Tali® Image-Based Flow Cytometer revealed that on an average the total concentration of cells or cell count of all the

biological and technical replicates ranged from 3 x10^6 cells/ml to 5x10^6 cell/ml. The average cell sizes measured by cytometer were 12-14µm (micrometers).

The cell viability test as performed by evaluating the percentage of live and dead cells revealed that insulin treatment for HG cells increased the cell survival with a significant ($p < 0.05$) increase in the percentage of live cell after 10 minutes, 1hour, 2hours and 4hours by 1.13, 1.1 ,1.13 & 1.13 folds (% of live cell after insulin treatment= 94±1.5, 93±1.5, 94±1.5 and 94±1.5) respectively as shown in the figure8. Equivalently, a corresponding 2.6,2.4, 2.6 &2.8 fold decrease (6.5± 1.5, 7± 1.5, 6.5± 1.5 & 6.5± 1.5) respectively in the number of dead cells were seen in treated cells as shown in figure 3.2. However, in comparison to the NG cell 24 hour HG cells, showed a significant reduction in live cells (92.5± 0.5 Vs 83± 0.5) with $p < 0.05$, as shown in figure 3.2 and an elevation in the percentage of dead cells (7.5 ± 0.5 Vs 17 ± 2). (Figure 3.2 A & B)

A. Live Cells

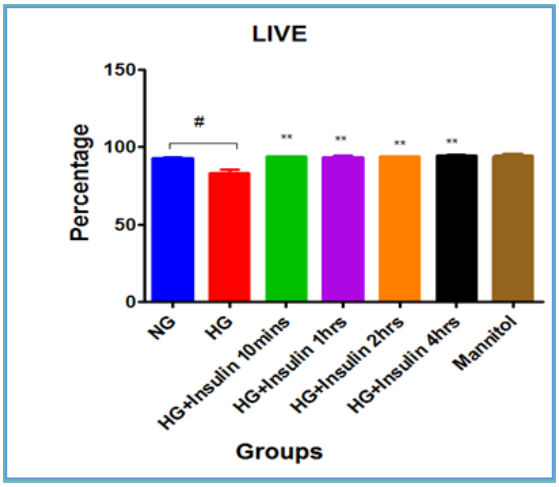

Figure 3.2 (A): Effect of insulin treatment on cell viability (live Cells). The percentage of live cells. Data are presented as means ±SD of 2-3 independent experiments analyzed by ANOVA with post-hoc

test for multiple experiments. * $p < 0.05$ compared within the HG group #$p < 0.05$ compared with NG, t-test.

B. Dead Cells

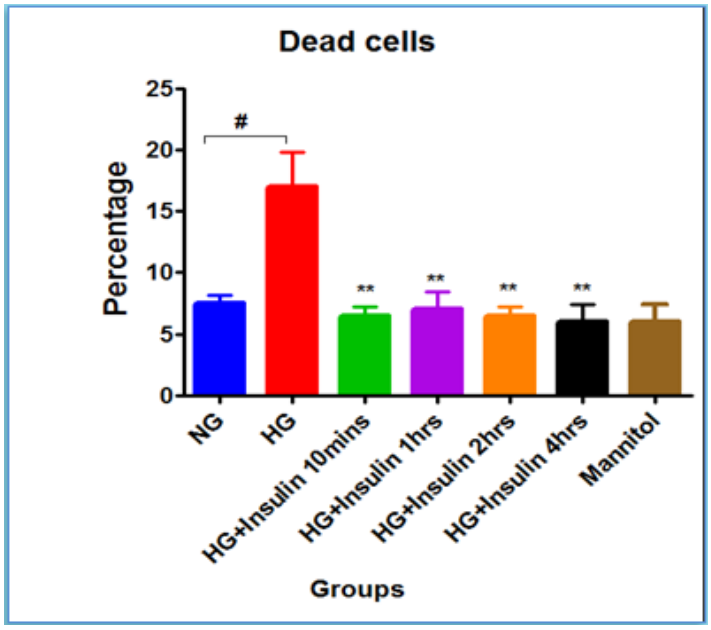

Figure 3.2 (B). Effect of insulin treatment on cell viability (Dead Cells). The percentage of Dead. Data are presented as means ±SD of 2-3 independent experiments analyzed by ANOVA with post-hoc test for multiple experiments. * $p < 0.05$ compared within the HG group #$p < 0.05$ compared with NG, t-test.

3.2.2 Cell cycle Analysis

Cell cycle analysis performed by Tali® Cell Cycle Kit revealed that neither high glucose nor insulin treatment affect the growth pattern of the cells or growth arrest. No significant difference was detected between NG cells, HG cells and after its treatment with insulin at different time points ($p > 0.05$) as shown in figure 3.2 (C).

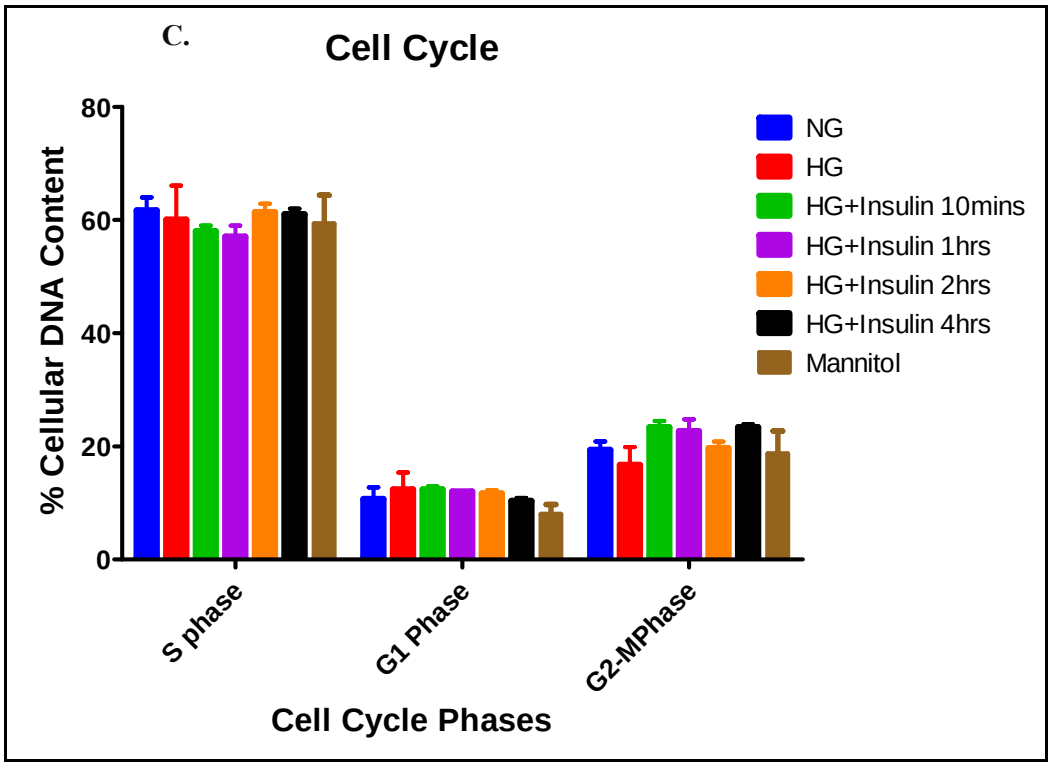

Figure 3.2(C), Cell cycle phases in HRECs under different conditions; NG (5mM glucose), HG (30mM glucose) and after insulin treatment to HG cells at 10 min, 1, 2, and 4 hours. Data are presented as Means ±SD of 2-3 independent experiments analyzed by ANOVA with post-hoc test for multiple experiments. Two-tailed p value is significant at $p \leq 0.05$.

3.3 Effect of high glucose and insulin on apoptosis and oxidative stress

To investigate whether insulin treatment to hyperglycemic cell induces a positive or negative impact on the rate of apoptosis HRECs were assessed for apoptosis using Tali Apoptosis Kit- Annexin V Alexa Fluor® 488 and Propidium Iodide. High glucose (30mM) significantly increased the number of the apoptosis in HRMECs by 3.8 folds, 2.25±0.48 Vs 8.75 ±1.109 (p value 0.0017). Contrary to this 100nM insulin treatment to HG cells causes a significant reduction in the number of the apoptotic cells in comparison to untreated HG cells after 10mins, 1hr, 2hrs & 4hrs of the insulin treatment by

1.7,1.5,1.6 & 2.3 folds with the corresponding *p values were 0.0094, 0.0275, 0.0161 and 0.0004, respectively as shown in figure 3.3.

A. B.

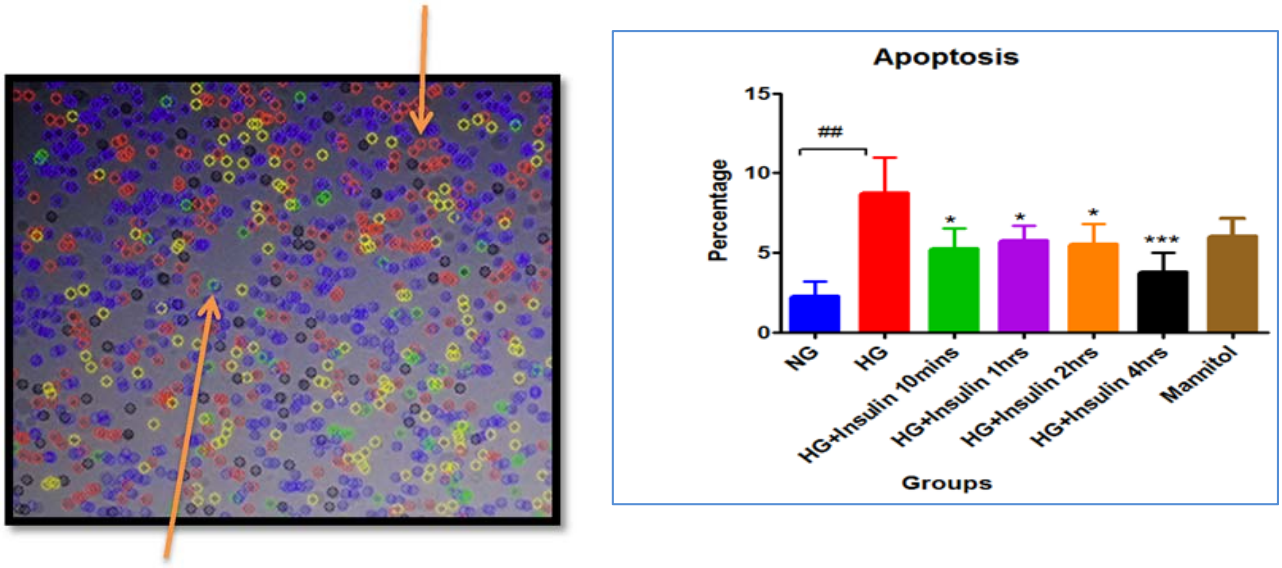

Figure 3.3. Effect of high glucose and 100nM insulin on apoptosis. Fig A, Annexin V and PI stained HRMECs shown by Tali® Image based cytometer whereas red spots indicates the numbers of deal cells , and green spots for apoptotic cells. B, Bars shows the data presented as Means ±SD of 2-3 independent experiments analyzed by ANOVA with post-hoc test for multiple experiments. Two-tailed p value is significant at $p \leq 0.05$. * $p < 0.05$ versus the untreated HG group, and #$p < 0.05$ compared with NG group..

Two independent techniques; Tali® CellROX® Oxidative Stress Reagents (quantitative assessment) and immunofluorescence (qualitative assessment) were used to examine the oxidative stress in HRMECs exposed to 5mM and 30mM glucose for 24 hours in comparison to HG cells treated with 100nM insulin. CellROX® Oxidative Stress analysis revealed a significant increase in the oxidative stress to cells exposed to high glucose in comparison to the cells under normoglycemic conditions (control group) by 2 folds(70.17 ± 5.160 Vs 35.67 ± 6.420) (#$p < 0.05$). Contrary to this finding 100nM insulin

treatment for 10 min, 1hrs, 2hrs & 4hrs resulted in a significant reduction in oxidative stress. The corresponding p values are 0.0393, and < 0.0001 for 10min and 1hrs,2hrs,4hrs, respectively as shown in (Figure 3.4 A, B).

Similar to the Tali® CellROX® results, a qualitative assay by the immunofluorescence utilizing H_2DCFDA dye exhibited a strong fluorescence in HRMECs exposed to high glucose compared to control cells. Evident weak signals were recorded with reduction in ROS spots upon insulin treatment in both the groups (NG and HG) in time based manner as shown in figure 3.4 C&D.

A. B.

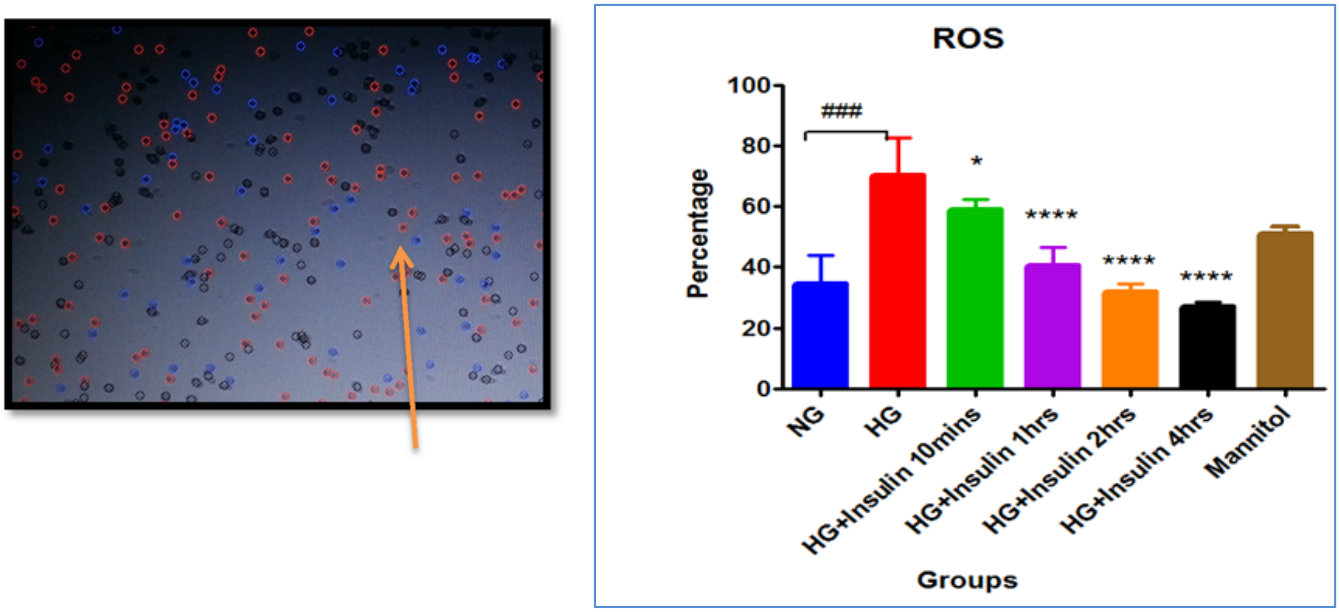

Figure 3.4. Effect of High glucose and 100nM insulin applications on ROS.. A, Tali® CellROX® Oxidative Stress Reagents stained HRMECs shown by Tali® Image based cytometer. B, Significant association between insulin treatment on HG cells and untreated HG cells to oxidative stress * $p < 0.05$ compared within the groups performed by One-way ANOVA; #$p < 0.05$ compared with NG, t-test.

Control

C.

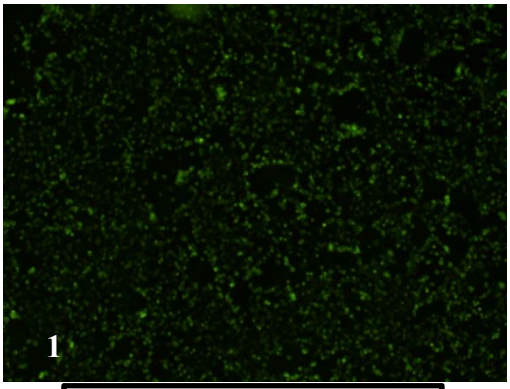

Control+1hour Insulin

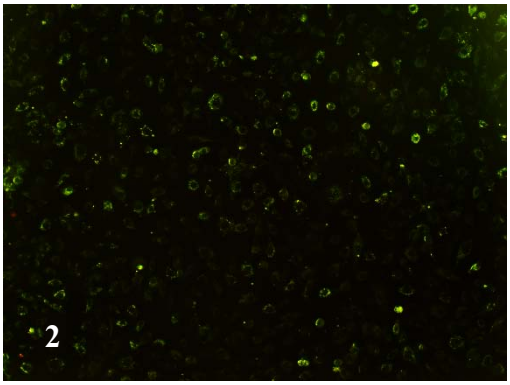

Control+2hour Insulin

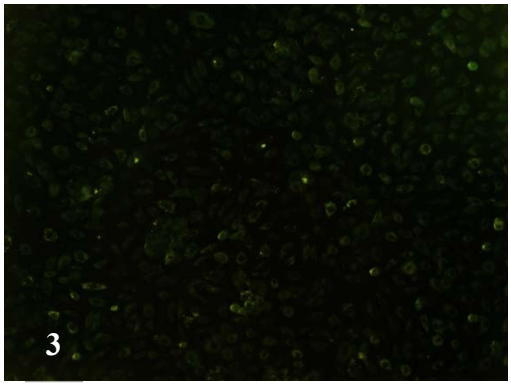

Control+4hour Insulin

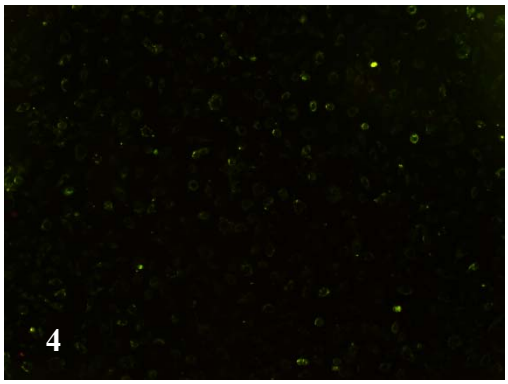

D.

High Glucose

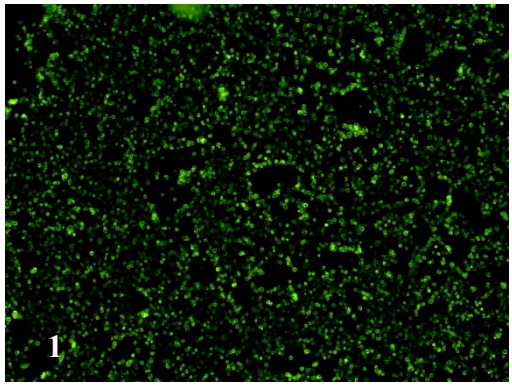

Glucose+1Hour Insulin

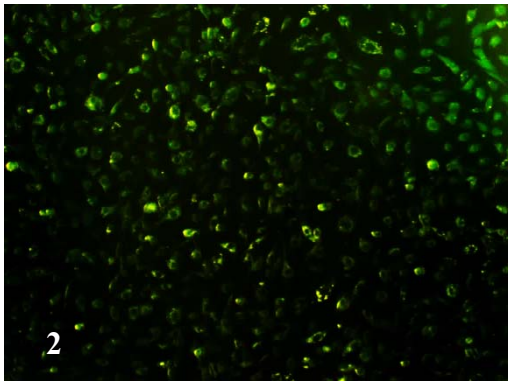

Glucose+2Hour Insulin

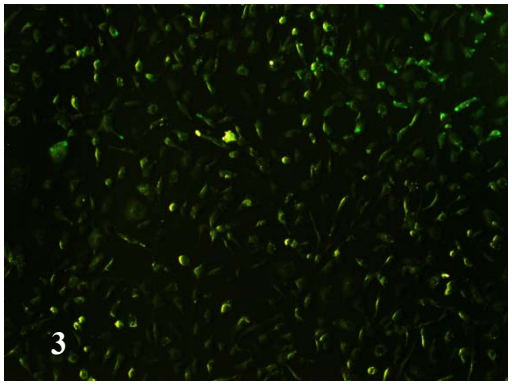

Glucose+4Hour Insulin

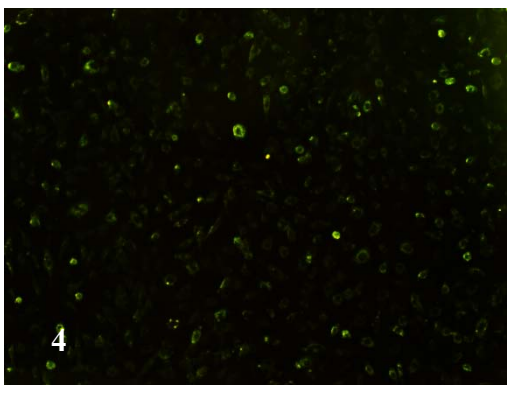

Figure 3.4 (C and D). Immunofluorescence for ROS production signal in each group shown in panel C and D.C1, HRMECs cultured in 5mM glucose. C2, HRMECs cultured in 5mM glucose and treated with 100nM Insulin for 1hrs. C3,5mM glucose and treated with 100nM Insulin for 2hrs. C4, 5mM glucose and treated with 100nM Insulin for 4hrs. D1, HRMECs cultured in 30mM glucose. D2, , HRMECs cultured in 30mM glucose and treated with 100nM Insulin for 1hrs. D3,30mM glucose and treated with 100nM Insulin for 2hrs. D4, 30mM glucose and treated with 100nM Insulin for 4hrs.

3.4 Effect of high glucose and insulin treatment on NO production

To study the effect of experimental hyperglycemia on NO production in HRMECs, treated with insulin at different time points the NO production in HRMECs cultured for 24hrs in 5 and 30mM glucose were examined by two independent parameters: Abcam's Nitric Oxide Fluorometric Assay Kit and DAF-FM and DAF-FM Diacetate Immunofluorescence dye.

Plot for the fluorescence vs. Pico moles nitrates were analyzed to determine the sample nitrite concentrations. Figure 3.5(A) illustrates the RFU (Relative Fluorescence vs Nitrite concentration (pmol/well/4hrs) for experimental standards to generate the relative concentration of the unknown samples.

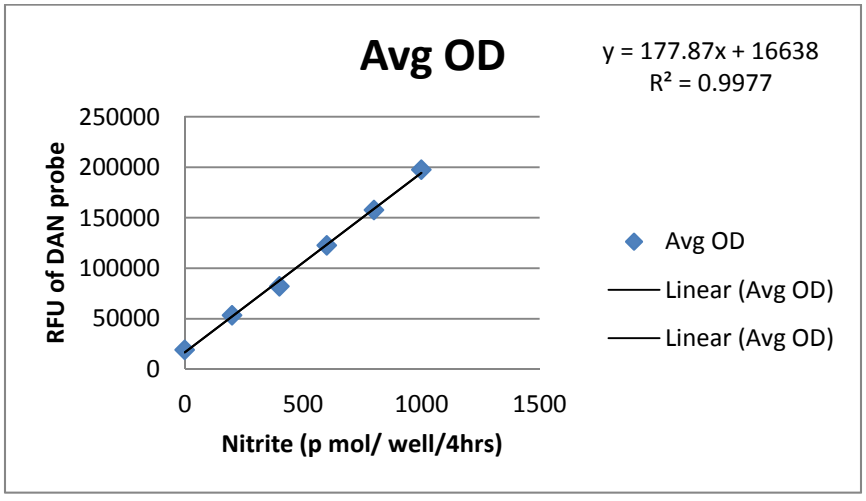

Figure 3.5(A): RFU (Relative Fluorescence vs Nitrite concentration (pmol/well/4hrs) for experimental standards to generate the relative concentration of the unknown samples

Table 3.1. Shows the calculated mean nitrite concentration of all samples:

Sample	**Nitrite Concentration in p mol**
NG (5mM glucose)	1.9
HG (30mM glucose)	6.4
HG+ Insulin 10mins	1.4
HG+ Insulin 1hrs	1.0
HG+ Insulin 2hrs	0.96
HG+ Insulin 4hrs	1.0
Mannitol	1.5
NG+ Insulin 10mins	2.4
NG+ Insulin 1hrs	1.0
NG+ Insulin 2hrs	1.3
NG+ Insulin 4hrs	1.4

The measurement of nitrite the oxidized product of NO was assayed by the fluorometric method revealed a significant increase in NO production in cells exposed to 30mM glucose compared to control exposed to 5mM glucose by ≈3.4 folds (1.9 ± 0.62 pmol/well/4hrs Vs 6.4 ± 0.78 pmol/well/4hrs, t-test) (# p value <0.05, p value: 0.0466) . However, when compared to 30mM glucose treated HRMECs, insulin- stimulated NO synthesis were significantly reduced at 10min, 1hrs, 2hrs & 4hrs of insulin treatment for both NG and HG groups. The corresponding *p value for all samples were <0.0001. In contrast, insulin had no significant effect on NO synthesis in HRMECs cultured in 30mM glucose in comparison to basal 5mM glucose.

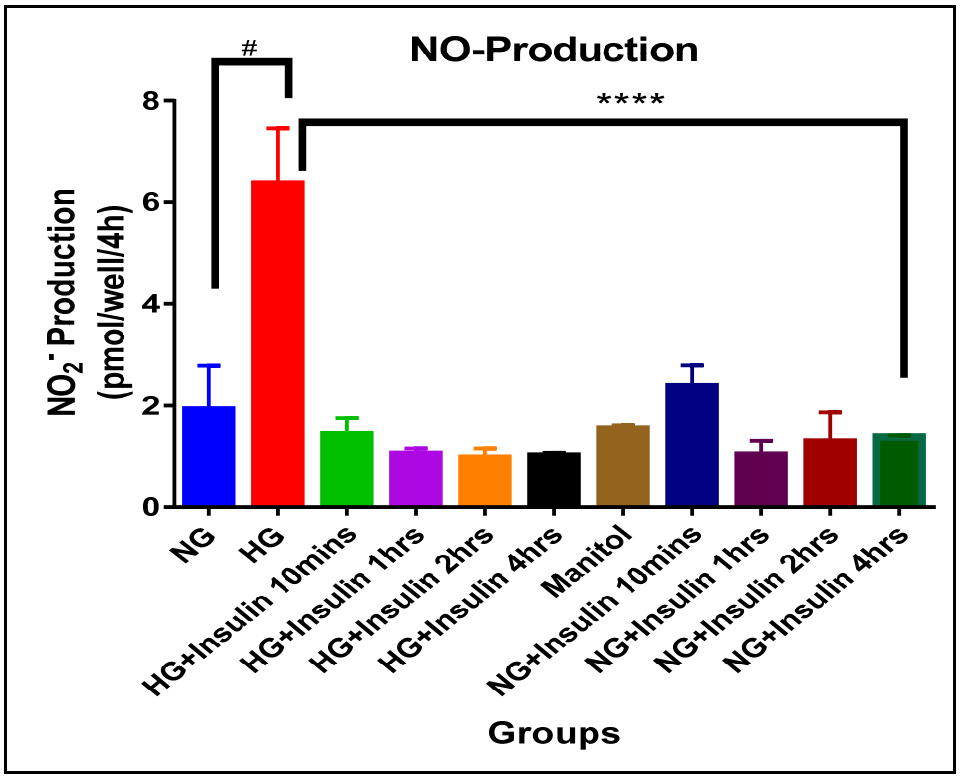

Figure 3.5(B). Insulin reduces glucose stimulated NO production in HG as well as NG cells. Bars shows the data presented as means ±SD of 2-3 independent experiments analyzed by ANOVA with Dennett's post-hoc test for multiple comparisons between individual groups. Two-tailed p value is significant at $p \leq 0.05$. **** $P < 0.05$ versus the untreated HG group, and #$p < 0.05$ compared with NG group

Significant association between insulin treatment on HG cells and untreated HG cells to NO * $p < 0.05$ compared within the groups performed by One-way ANOVA; #$p < 0.05$ compared with NG, t-test.

Immunofluorescence staining with DAF-FM diacetate immunofluorescence dye were performed and in confirmation showed similar findings with the above fluorometric assay results. Immunofluorescence results showed strong RNS signals with HG cells which decreases and gave week signals for RNS with insulin treated cells as evident in the figure 3.5(C &D).

Control

C.

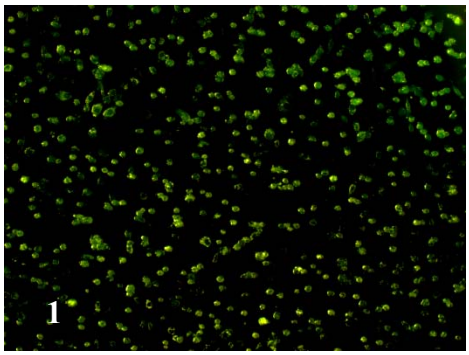

Control+1hour Insulin

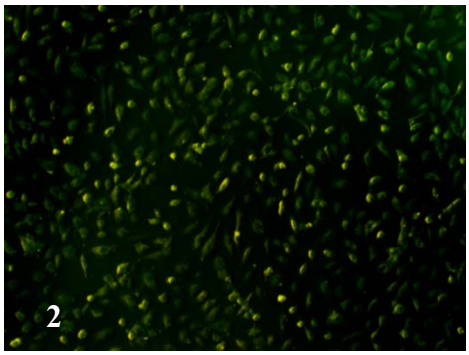

Control+2hour Insulin

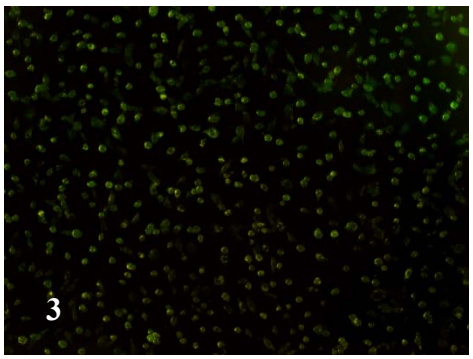

Control+4hour Insulin

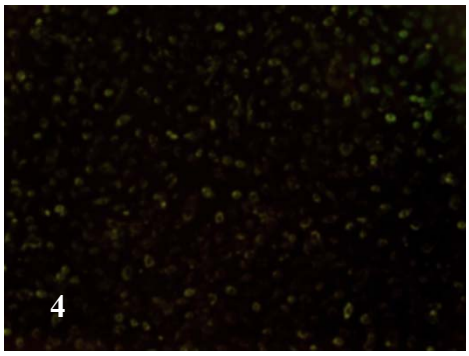

High Glucose

D.

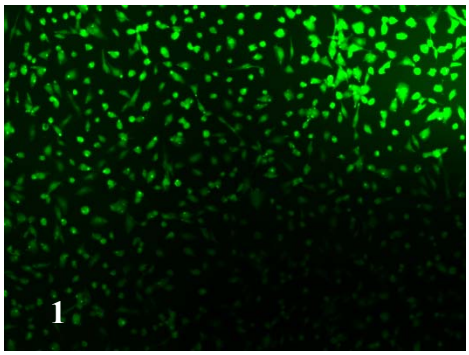

Glucose+1Hour Insulin

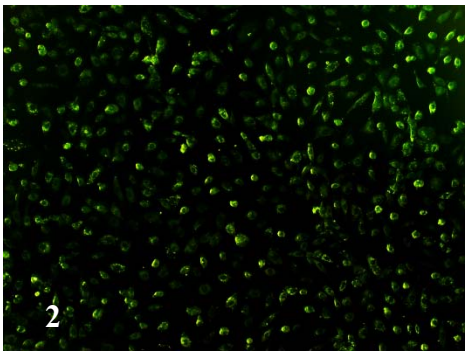

Glucose+2Hour Insulin

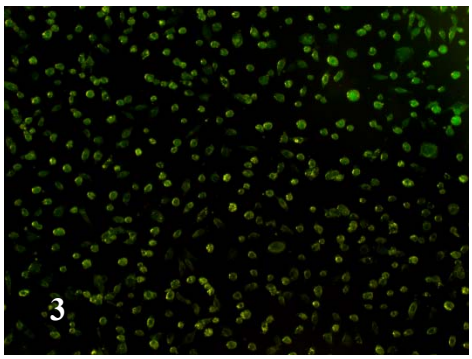

Glucose+4Hour Insulin

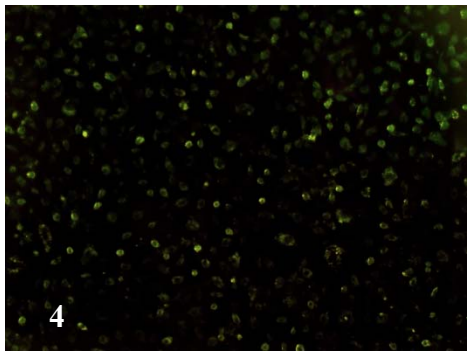

Figure3.5 (C&D). Immunofluorescence for RNS production signal in each group in two panels C: NG group and D: HG group. C1, HRMECs cultured in 5mM glucose. C2, HRMECs cultured in 5mM glucose and treated with 100nM Insulin for 1hrs. C3,5mM glucose and treated with 100nM Insulin for 2hrs. C4, 5mM glucose and treated with 100nM Insulin for 4hrs. D1, HRMECs cultured in 30mM glucose. D2, , HRMECs cultured in 30mM glucose and treated with 100nM Insulin for 1hrs. D3,30mM glucose and treated with 100nM Insulin for 2hrs. D4, 30mM glucose and treated with 100nM Insulin for 4hrs.

3.5 PI3K/Akt pathway, eNOS, VEGF-A, and NFKB gene expression analysis

To investigate the inhibitory effect of insulin on NO production gene expressions of IRS-1,IRS-2,PI3K,Akt and eNOS involved in the PI3K/Akt insulin signaling pathway were analyzed using specific primers as stated earlier and against UBC as housekeeping control gene. Prior to mRNA expression analysis, RNA purity and concentrations for each sample was spectrophotometrically evaluated using Nano drop. The Table 3.2 below show records of the RNA concentration and purity:

Table 3.2. RNA concentration and Purity

Sample	**RNA quantity (ng/µl)**	**RNA purity (260/280)**
NC	671.4	1.80
HG	882	1.82
HG+INS10min	792	1.89
HG+INS1Hrs	1095.2	1.94
NG+INS10min	708.3	1.93
NG+INS1Hrs	859	1.94

To test the effect of glucose and insulin at different time point on PI3K/Akt pathway, HRMECs were exposed to 5mM or 30mM glucose for 24 hours followed by 100nM insulin treatment for 10mins and 1hrs followed by RNA extraction and cDNA preparation based on RNA concentrations.

Real Time RT-PCR expression analysis of IRS-1 mRNA in HRMECs exposed to 5 or 30mM glucose revealed no significant change in the expression levels. However, insulin treatment of HG cells for 1hr produced a significant upregulation of IRS-1 mRNA gene expression with ≈97 fold increase p value 0.0002 as shown in Figure 3.6(A). Similar to IRS-1 gene expression, IRS-2 mRNA gene expression was significantly increased by ≈139 fold with 1hrs of insulin treatment in HG cells [30mM glucose for 24h] with a p value of 0.0049. Control cell [NG] exposed to 5mM glucose for 24hrs when treated with 10mins insulin resulted in ≈112 fold increase in IRS-2 gene expression with p value 0.0143. IRS-1, IRS-2 gene expressions are not significantly different between HG and NG groups as shown in (Figure 3.6B).

A.

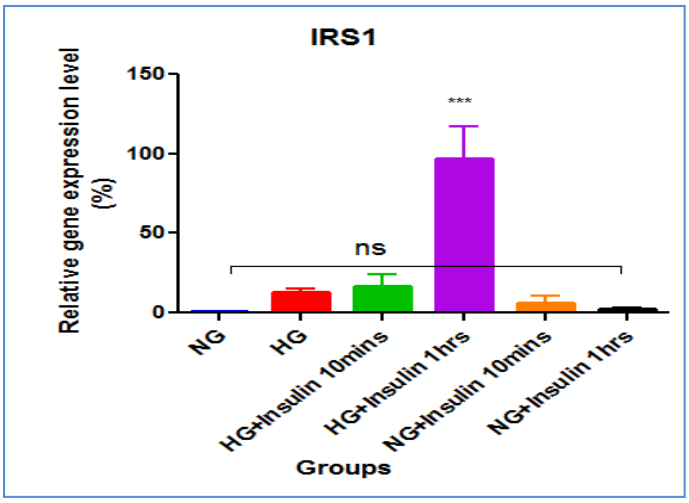

Figure3.6(A): Real Time quantitative RT-PCR analysis of IRS-1 in RNA extracts of HRMECS exposed to 5 or 30mM glucose for 24hrs followed by 100nM insulin treatment for 10mins and 1hrs. Bars shows the data presented as means ±SD of 2-3 independent experiments analyzed by ANOVA with Dennett's post-

hoc test for multiple comparisons between individual groups. Two-tailed p value is significant at $p \leq 0.05$. **** $P < 0.05$ versus the untreated HG group, and **$p < 0.05$ compared with NG group

B.

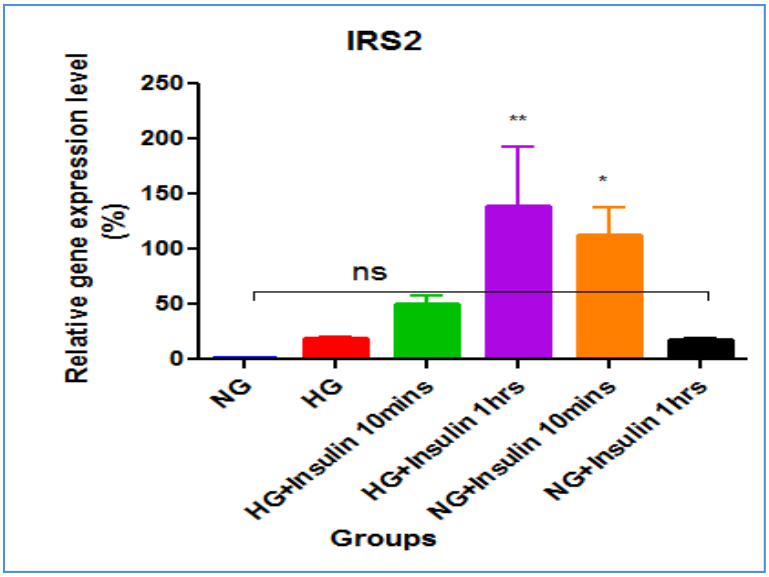

Figure3.6(B): Real Time quantitative RT-PCR analysis of IRS-2 in RNA extracts of HRMECS exposed to 5 or 30mM glucose for 24hrs followed by 100nM insulin treatment for 10mins and 1hrs. Bars shows the data presented as means ±SD of 2-3 independent experiments analyzed by ANOVA with Dennett's post-hoc test for multiple comparisons between individual groups. Two-tailed p value is significant at $p \leq 0.05$. **** $P < 0.05$ versus the untreated HG group, and **$p < 0.05$ compared with NG group

The mRNA expressions of PI3K, Akt and eNOS respectively showed a significant upregulation in expression following 24hrs HG exposure by 4.2, 1.6 and 8.7 folds, compared to cells exposed to 5mM glucose group with the corresponding p values are 0.0072, 0.049 and 0.018 respectively as shown in Figure3.6(C, D &E).

C.

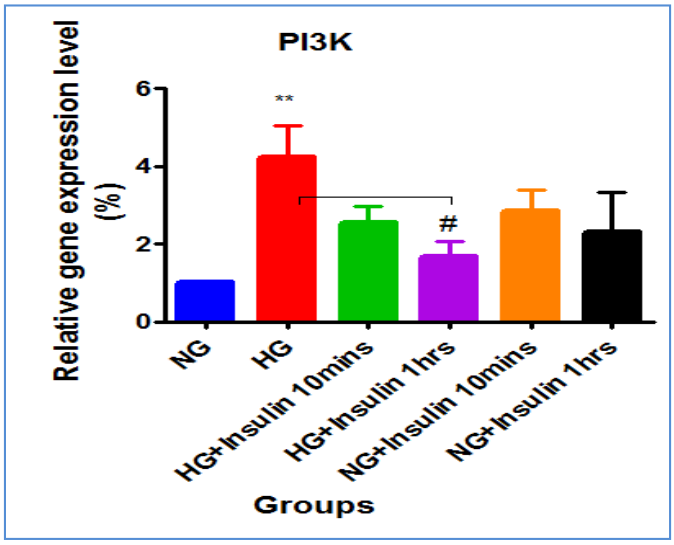

Figure 3.6 (C): Real Time quantitative RT-PCR analysis of PI3K in RNA extracts of HRMECS. Two independent biological samples with three technical replicates analyzed. *p value < 0.05 for differences between control, HG and insulin treated HRMECs were considered significant.

D.

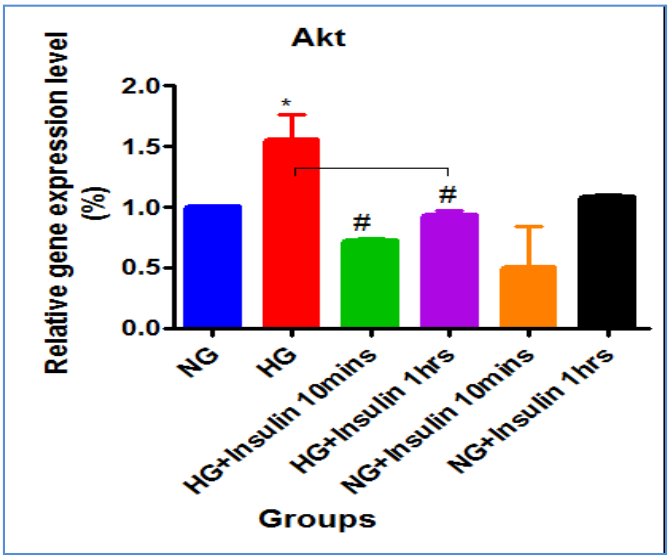

Figure 3.6(D): Real Time quantitative RT-PCR analysis of Akt (D) in RNA extracts of HRMECS exposed to 5 or 30mM glucose for 24hrs followed by 100nM insulin treatment for 10mins and 1hrs. Two independent biological samples with three technical replicates analyzed. *p value < 0.05 for differences between control, HG and insulin treated HRMECs were considered significant.

E.

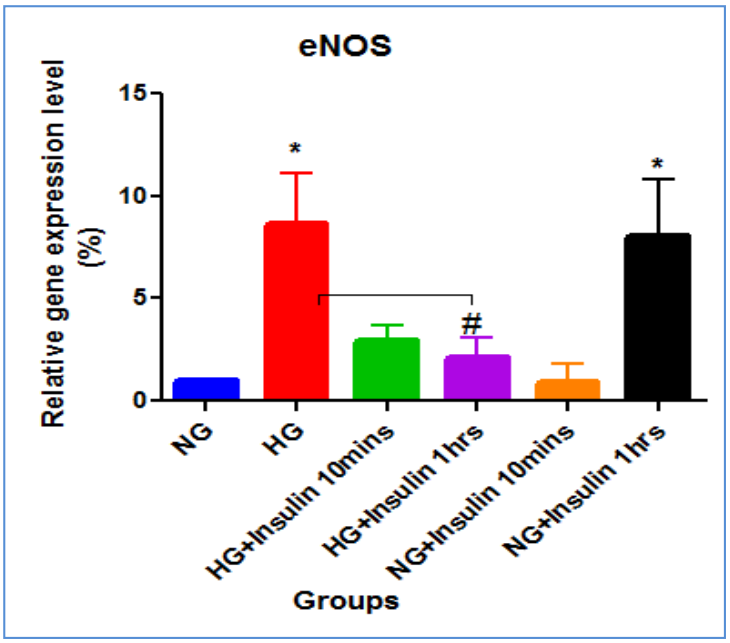

Figure 3.6(E): Real Time quantitative RT-PCR analysis of eNOS (E) in RNA extracts of HRMECS exposed to 5 or 30mM glucose for 24hrs followed by 100nM insulin treatment for 10mins and 1hrs. Two independent biological samples with three technical replicates analyzed. *p value < 0.05 for differences between control, HG and insulin treated HRMECs were considered significant.

In an attempt to investigate the differences between HRMECs culture in either glucose concentrations and HG treated with insulin that could be correlated to gene expression analysis and attenuated NO production western blot for IRS-1 and PI3K proteins was performed . Prior to SDS-PAGE the concentration of the protein in each sample was determined using TECAN® ELISA to establish the minimum viable concentration to be used. Plot for the absorbance vs BSA standard concentration were analyzed to determine the protein concentration. Figure3.7(A) . illustrates the absorbance Vs concentration for the experimental standard to generate the relative concentration of the unknown samples.

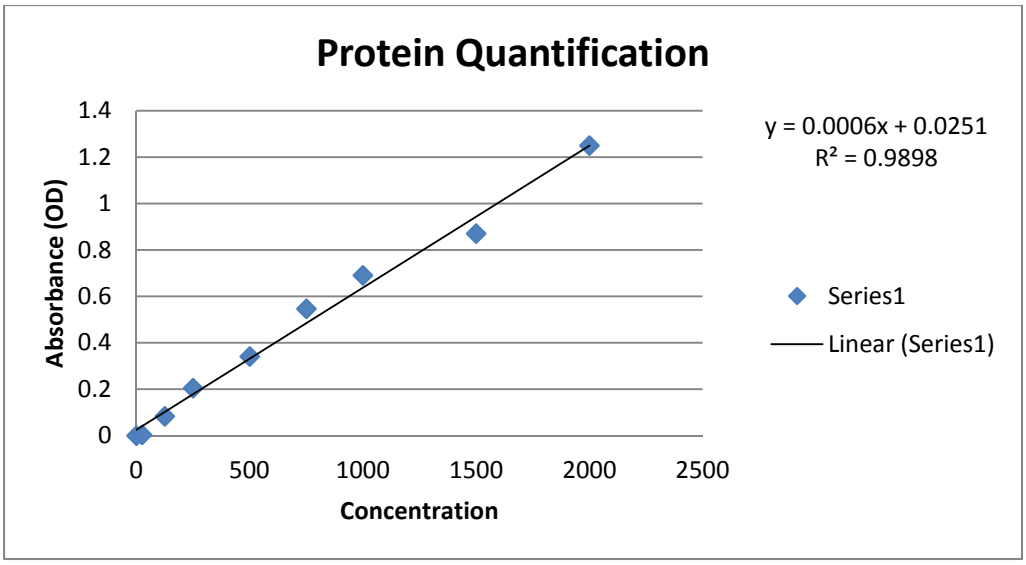

Figure3.7(A). Protein quantification

Table3.3: Average calculated protein concentrations of the samples.

Sample	Protein Concentration in ng	50ng Protein Volume (µL)
NG (5mM glucose)	2629.5	25
HG (30mM glucose)	2009.5	27
HG+ Insulin 10mins	1719	25
HG+ Insulin 1hrs	1588.167	26
HG+ Insulin 2hrs	1498.167	27
HG+ Insulin 4hrs	2769.5	22
NG+ Insulin 10mins	2322	26
NG+ Insulin 1hrs	2084.5	25
NG+ Insulin 2hrs	2204.5	26
NG+ Insulin 4hrs	2514.667	21

Quantitative analysis of Western blots illustrated that there was no significant difference in expression of IRS-1(165kDa) in HRMECs cultured in either 5 or 30mM

glucose.(Figure3.7 B) However, a significant band was visual with 4hrs insulin treatment of 24hrs HG cells with ≈8 fold increase with 4hrs of insulin, p value 0.0003. PI3K (85kDa) did not give specific band, this could have been due to high concentration of protein used therefore, a plan to perform immunoprecipitation of these protein will be attempted.

I.

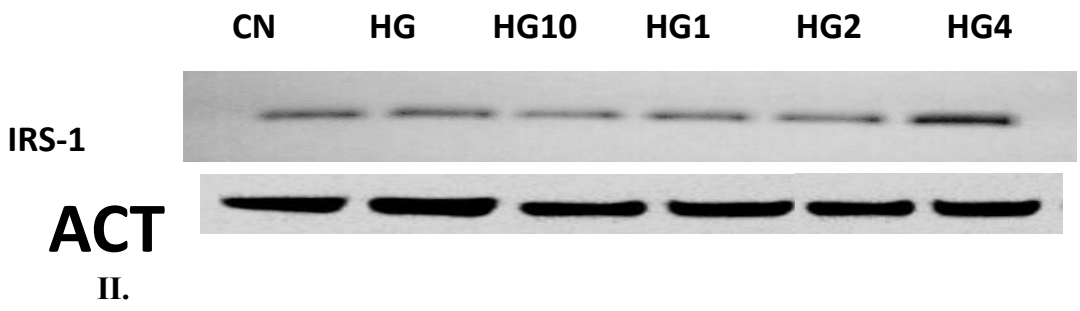

II.

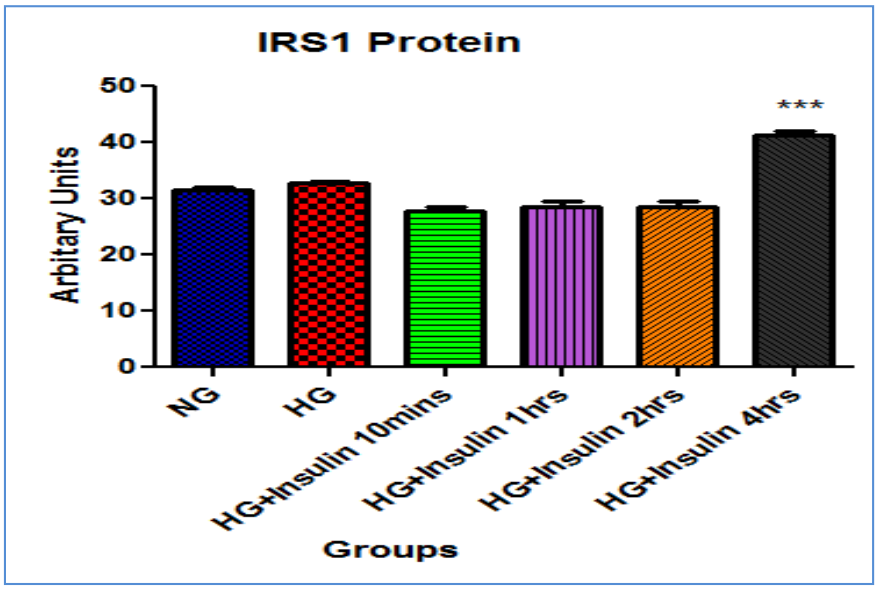

Figure3.7(B). Effects of glucose concentrations and insulin treatment on expression of IRS isoform. I &II, HRMEC lysate were prepared from cells cultured for 24hrs in medium containing 5mM and 30mM glucose and insulin treatment for 10min, 1hrs, 2hrs and 4hrs respectively. SDS-PAGE resolved lysate were transferred to nitrocellulose and probed with antibodies indicated.

3.6 Hyperglycemia stimulates VEGFA expression

3.6.1 VEGFA and NFkB gene expression

To investigate angiogenesis and apoptosis in a progressive obliteration of DR, genes involved in angiogenesis such as VEGF-A and proapoptotic gene such as NFkB were assessed by Real Time RT-PCR. The relative quantitative mRNA gene expression of VEGF-A gene in HRMECs exposed to 30mM glucose showed a significant upregulation of the expression compared to the cells exposed to 5mM glucose with ≡227 fold increase and p value of 0.0008 as shown in (Figure 3.8 A). The analysis of proapoptotic gene NFkB however, showed no difference between cells exposed to HG with cells exposed to normoglycemia and even treated cells with insulin under normoglycemia and hyperglycemic conditions (*p value < 0.05) as shown in (Figure3.8B)

A.

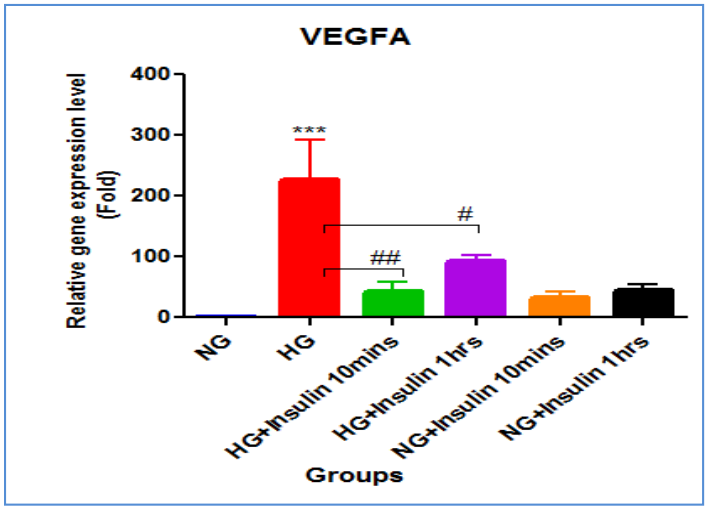

Figure3.8 (A). Real Time quantitative RT-PCR analysis of VEGFA (F) in RNA extracts of HRMECS exposed to 5 or 30mM glucose for 24hrs followed by 100nM insulin treatment for 10mins and 1hrs. Two independent biological samples with three technical replicates analyzed. *p value < 0.05 for differences between control, HG and insulin treated HRMECs were considered significant.

B.

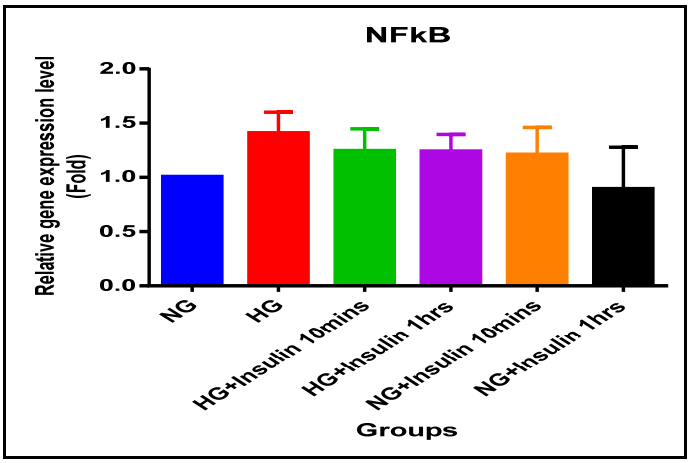

Figure3.8(B). Real Time quantitative RT-PCR analysis of NFkB (B) in RNA extracts of HRMECS exposed to 5 or 30mM glucose for 24hrs followed by 100nM insulin treatment for 10mins and 1hrs. Two independent biological samples with three technical replicates analyzed. *p value < 0.05 for differences between control, HG and insulin treated HRMECs were considered significant.

3.6.2 Effect of HG and insulin treatment on VEGF-A Protein

Protein expression analysis of the angiogenesis protein VEGFA was performed by ELISA in order to correlate the findings with gene expression results. ELISA results showed that the VEGFA protein expression in 24hrs HG exposed cell was significantly elevated by 0.16 fold than those of the NG exposed cells (p value 0.0374). In the insulin treated cells a significant increase in the VEGFA protein expression was recorded in 24hrs HG exposed cells treated with 100nM insulin for only 1hrs and 4hrs by 0.26, 0.25 fold in comparison to control cell with corresponding significant p values of <0.0001, respectively. The VEGFA protein expression in 24hrs 5mM glucose exposed cell treated with 100nM insulin also showed similar pattern of protein expression with significant elevated expression only at 1hrs and 4hrs by 0.21 and 0.23 folds with p values were

<0.0001, respectively. The figure3.9 below illustrates the VEGFA protein expression in HRMECs.

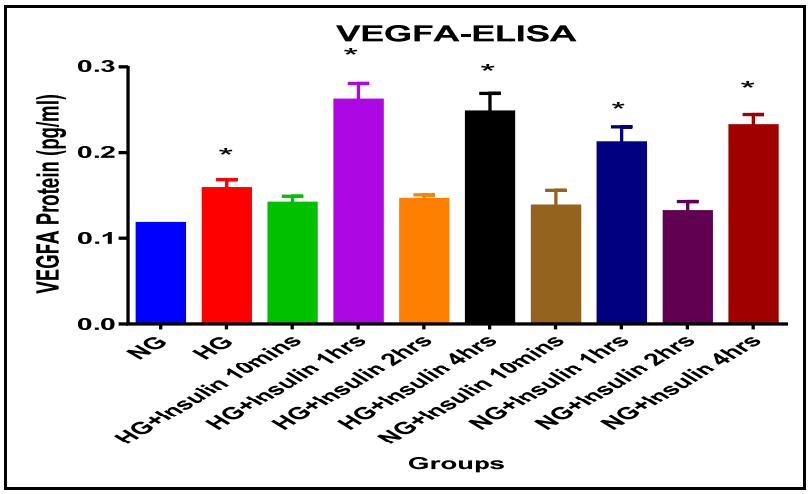

Figure3.9. The ELISA examination of VEGF protein expression in HRMECs. The treated cells showed an increased VEGFA protein expression in both high glucose, insulin treated and high glucose-insulin treated cell. *p value < 0.05 for differences were considered significant.

3.7 Insulin attenuates HRMECs barrier function

To evaluate whether insulin had an effect on the migration of HRMECs, an in vitro scratch wound test was performed to measure the migration ability of HRMECs at 5mM and 30mM glucose with and without 100nM insulin was performed. As shown in the Figure 3.10, a significant wound closure was observed in the group treated 24hrs with 30mM glucose compared to 5mM treated group. However, the HRMECs with 24hrs high glucose and low glucose exposer followed by co-treatment with 100nM insulin showed wider wound area when assessed after 4hrs, 8hrs and 12hrs. These results indicate that insulin could effectively significantly inhibit HG exposed HRMECs migration ability as shown in (Figure3.10A,B).

Control

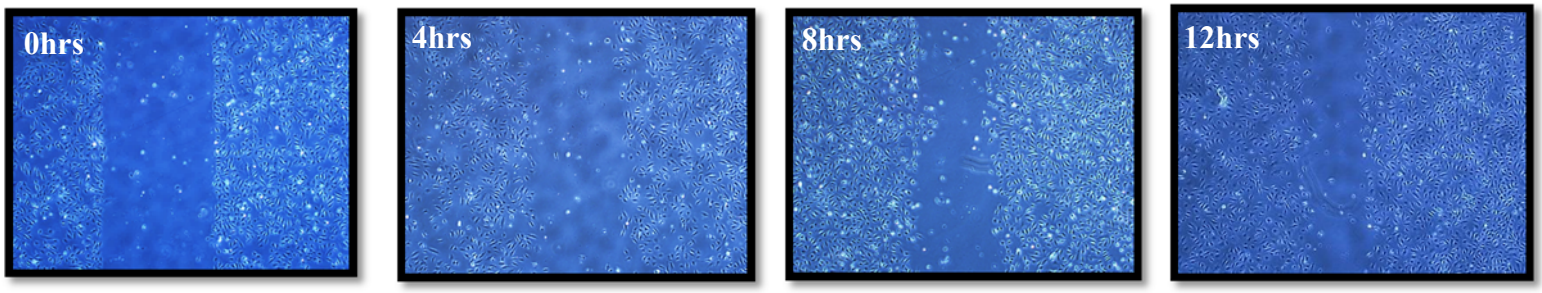

Control + Insulin

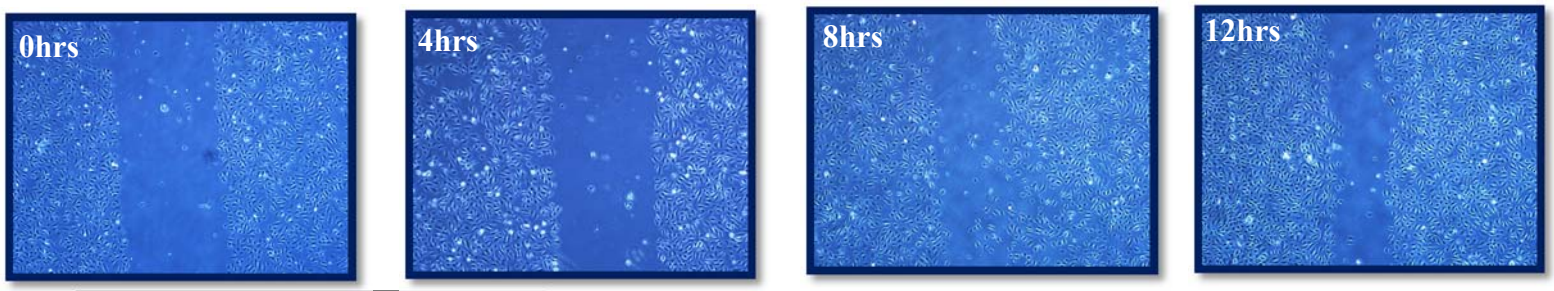

High Glucose

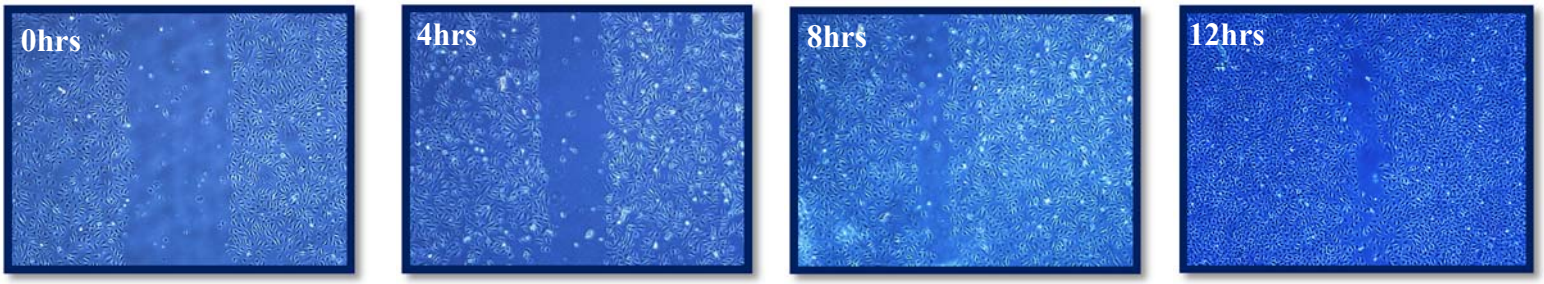

High Glucose +Insulin

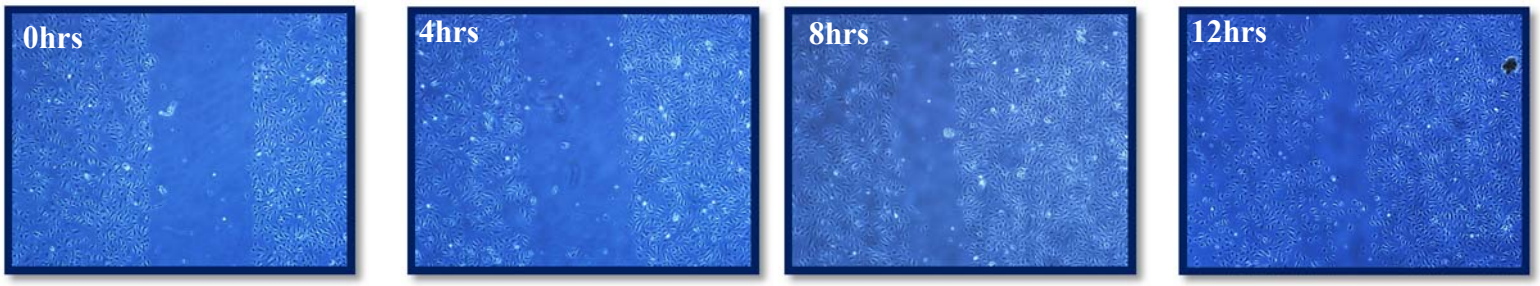

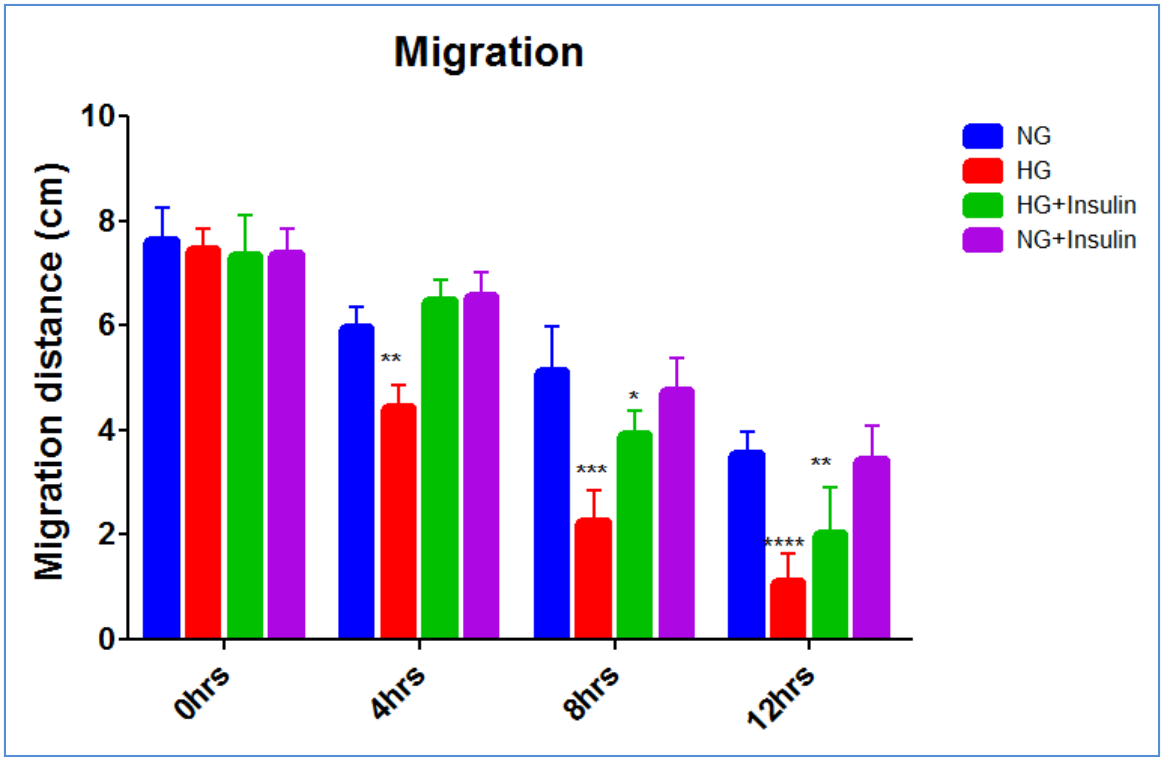

Figure3.10. Insulin inhibited HRMEC migration induced by high glucose. A, HRMECs photographed for re-endothelialization after wound scratch created by 1000µl pipette. B, The quantitative data of migration distance were from two independent experiments. Bars shows the data presented as means ±SD of 2-3 independent experiments analyzed by ANOVA with Dunnett's post-hoc test for multiple experiments. Two-tailed p value is significant at $p \leq 0.05$. * $p < 0.05$ versus the untreated HG group, and #$p < 0.05$ compared with NG group.

3.8 Insulin down regulates adhesion molecule P-selectin in HRMECs

To assess whether insulin had an effect on the cellular adhesion molecules P-selectin and ICAM-1 in HRMECs, protein expression was measured using BD® Acuri flow cytometer. As shown in the figure 15, the flow cytometry results revealed a significant increase in the P-Selectin expression in 24hrs HG exposed cell compared to NG cell with ≈12 fold increase and p value 0.0022. The expression pattern under the effect of insulin treatment in 24hrs NG followed by 100nM insulin treatment revealed a gradual

significant increased expression from 10mins to 1hrs and 2hrs however, no significance was encountered with 4hrs insulin treatment in control group treated with insulin. Contrary to this finding although 24hrs HG cells treated with insulin for 10mins, 1hrs and 2hrs had significant increase by ≡20, 17 & 11 folds for P-selectin expression (p = <0.0001), and there was a gradual significant decrease in the expression at 4hrs by 8.6 fold. Consistent with this result ICAM-1 expression was significantly decreased in 24hrs HG exposed cells treated with insulin for 4hrs by ≈1.3 folds with p value 0.003. Figure3.11.

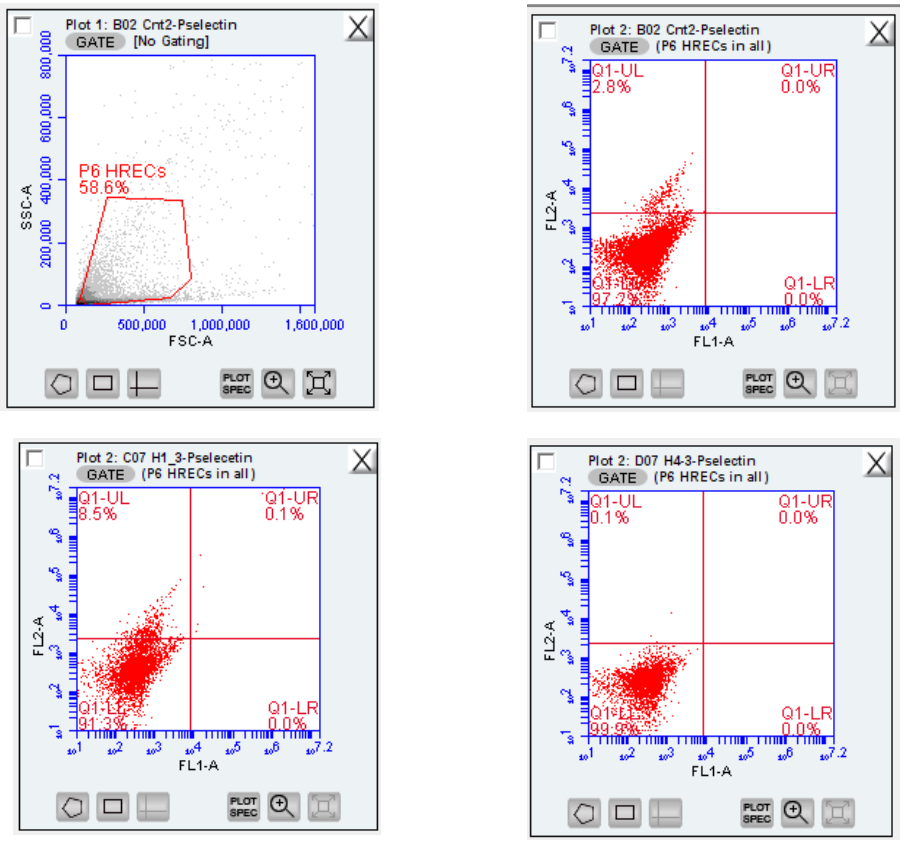

Figure3.11.Treatment of hyperglycemic HRMECs with insulin significantly reduced expression of adhesion proteins P-selectin and ICAM-1. A, Demonstrates the normal distribution of the unstained HRMECs for gating based on cell size and morphology, the variation in the distribution of the HRMECs depending on glucose exposure and insulin treatment.

B.

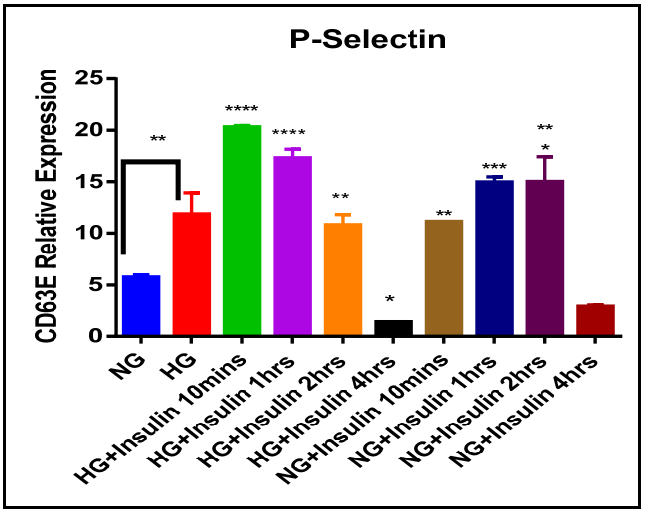

Figure3.11(B).Treatment of hyperglycemic HRMECs with insulin significantly reduced expression of adhesion proteins P-selectin and ICAM-1. B, Statistical analysis of the FACS results using one way ANOVA *p values < 0.05 were considered significant.

C.

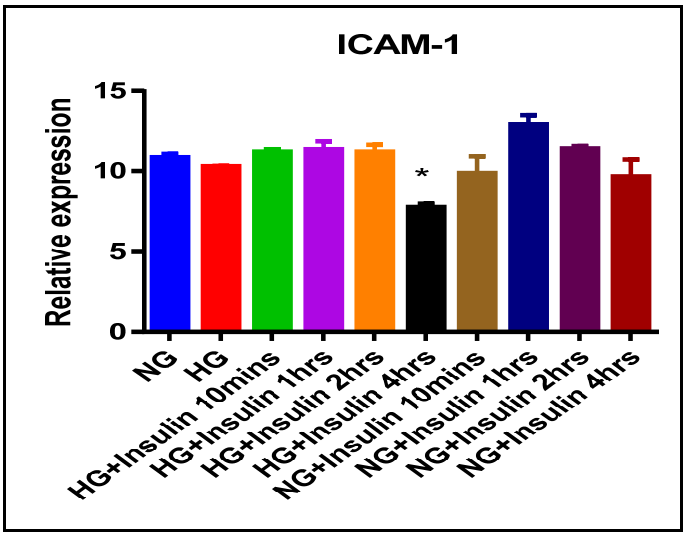

Figure3.11(C).Treatment of hyperglycemic HRMECs with insulin significantly reduced expression of adhesion proteins P-selectin and ICAM-1. C, Statistical analysis of the FACS results using one way ANOVA *p values < 0.05 were considered significant.

CHAPTER 4

DISCUSSION

4.1. DISCUSSION

The vascular endothelium maneuvers a crucial role in the maintenance of vascular health by regulating various factors such as vascular tone, platelet aggregation, coagulation and monocyte adhesion, amongst others. The mechanism of endothelial vascular tone regulation occurs through the coordinated secretion of endothelial vasodilators and vasoconstrictors. Abnormal vascular endothelial function, as defined by the decrease bioavailability of the principal vasodilator NO produced by the endothelium NOS and in cases of insulin resistance are well described in in vivo and in vitro studies with type 1, type2 diabetes and cardiovascular disorders (Salt et al., 2003; Wheatcroft, Williams, et al., 2003). Insulin stimulated NO productions are reported to be well established in cardiovascular and macrovascular endothelium and its association with PI3K/Akt pathway (Montagnani et al., 2001). Contrary to this insulin signaling in retinal endothelium have minimal reports with some studies suggesting it to be an important physiology player in hyperglycemia or insulin resistance induced DR (Reiter & Gardner, 2003). This prompted us to investigate the association between hyperglycemia and insulin mediated PI3K/Akt pathway eNOS directed NO production and associated multivariate effect on HRMECs survival, proliferation, angiogenesis, adhesion, apoptotic and inflammatory markers.

The present study demonstrates a number of important findings that contributes to the understanding the role of hyperglycemia and insulin-resistance in human retinal endothelial cell homeostasis. The key findings of the study include:

Hyperglycemia causes an increase in ROS/oxidative stress and apoptosis, while insulin promotes a significant decrease in ROS and apoptosis. These results are consistent with previous studies done on BRECs and mice RECs exposed to 5 and 25mM glucose however, these studies were performed on long term glucose exposure for 5 days (Madsen-Bouterse & Kowluru, 2008). The mechanism for increase ROS in hyperglycemic cells remain unclear however, studies suggest increased glycolytic pathway flux, cytosolic NADH and inflammation among other to induced mitochondrial ROS production (Madsen-Bouterse & Kowluru, 2008).

In vivo studies on diabetic animals suggest a reduction in oxidative stress upon administration of antioxidants such as Vitamin E and aspirin among others thereby significantly reducing DR (Kowluru et al., 2001). Other studies reported that oxidative stress a leading cause of insulin resistance (Bloch-Damti & Bashan, 2005). However, all these studies do not report the effect of insulin for the reduction of ROS. The current study reports that short acting insulin treatment of 24hrs HG exposed HRMECs significantly reduced ROS production consistent with previous studies (Bloch-Damti & Bashan, 2005; Kowluru et al., 2001).

eNOS mediated NO production increases with hyperglycemia but remarkably decreases with insulin treatment after 1hour, 2 hours and 4 hours. The productions of NO in response to high glucose concentration are quite contradicting among multiple studies. Cosentino et al. (1998) reported a significant elevation of NO production in HAECs exposed to high glucose for 5 days, contrary to this under similar conditions salt et la. (2003) reported a reduction in NO. Similar results are also reported in bovine retinal endothelial cells exposed to 25mM glucose for 5 days (Chakravarthy et al., 1998;

Cosentino, Hishikawa, Katusic, & Lüscher, 1997; Salt et al., 2003). Human aortic endothelial cells under similar conditions had elevated NO production (Cosentino et al., 1997). The current study reports a significant increase in NO production in HRMECs exposed to 24hrs 30mM glucose. The dissimilarity with the above mentioned bovine retinal endothelial cells study could be due to different endothelial cell types used or varied duration of experimental hyperglycemia. The most significant reason for the variation may be due to different method of NO measurement where, the above mentioned studies measured NO production by isolated NO meters. However, in the current study fluorometry a more sensititve method to measure oxidized product of NO, nitrite an indicator direct NO production was utilized and confirmed by the immunoflouresence technique using the dye DAF-FM Diacetate. Cosentino et al. have reported a significant increase in NO production in aortic endothelial cells exposed to high glucose for 5 day using flurometric nitrite measurment method (Cosentino et al., 1997) which is similar to our findings. Therfore, the results of the present study could be justified.

Gene and protein expression analysis of PI3K/Akt pathway. This this study it demonstrates a slight increase but insignificant elevation of IRS-1 and IRS-2 genes expression in hyperglycemic condition compared to the basal control condition, while gene expression of PI3K, Akt and eNOS were significantly elevated in the presence of high glucose. Insulin treatment caused an up regulation of IRS-1 and IRS-2 genes after 1 hour however, PI3K, Akt and eNOS were significantly reduced. Confirming the gene expression, western blot revealed no significant change in the lysate protein expression of IRS-1 in 24hrs HG exposed cells, 10mins, 1hrs and 2hrs insulin treated cell. However,

significant increase in IRS-1 protein expression was evident in 24hrs HG cell treated with insulin for 4hrs. These results are consistent with previous in vivo studies on rat retinal cells exposed to high glucose for 5 days and 100nM insulin treatment. They reported that diabetic rats had elevated basal PI3K and down regulated IRS-2. However, consistent with the western blot results of this study the IRS-1 protein level remains unchanged compared to basal control group . They report a significant restoration of IRS-1 protein expression upon insulin treatment a result consistent with the findings of this study (Reiter et al., 2006). Reiter et al. study reported that the protein analysis of the PI3K/Akt signaling pathway however, in the current study similar pattern of result had been also shown at the gene expression as well, where the gene expression of PI3K were upregulated with no significant change in IRS-1 expression. The protein expression of IRS-1 showed increased expression after 4 hours insulin treatment. The variation is some results such as reported earlier the current study showed reduced Akt expression followed by restoration after insulin treatment could be due to difference in the tissue type, varied duration of experimental hyperglycemia and because the gene expression are noted to different to protein expression. This study also reports a significant elevation in IRS-2 and eNOS gene expression in control group exposed to insulin treatment suggesting that insulin to be a positive regulator of PI3K/Akt signaling. However, further investigation needs to be done to investigate the effect of insulin on normal and hypoglycemic cell to prove the finding.

The analysis of angiogenic and proapoptotic markers VEGFA and NFkB by RT-PCR showed no significant change in the expression of NFkB in hyperglycemic alone, hyperglycemic and normoglycemic cells with insulin treatment at all-time points.

However, hyperglycemia significantly increased the expression of VEGF. Though compared to basal control group insulin treatment significantly increased the expression of VEGFA in both hyperglycemic and normoglycemic cells yet the expression was low compared to HG state at both gene and protein levels. Consistent with the VEGFA gene expression HG significantly increased the increase the cell migration and angiogenesis while insulin treatment significantly improves barrier function. Consistent with the study done on bovine retinal endothelial cell (Wu et al., 2010) , this study found that the combined effect of glucose and insulin was weaker than that of the glucose alone .

Previous studies suggest that PI3K inhibitors inhibit insulin-induced VEGF expression(Wu et al., 2010). In this study, the results are consistent with earlier studies as stated earlier high glucose and insulin resistance inhibits insulin induced PI3K , eNOS expression thereby inhibiting the insulin-stimulated PI3K insulin signaling pathway and nitric oxide production in HRMECs. Therefore, it can be proposed that high glucose could inhibit insulin-induced VEGF expression through impaired PI3K signaling pathway.

Hyperglycemia significantly increases adhesion protein P-selectin with significant reduction at 4hrs insulin treatment. Increased adhesion molecules are reported to increase endothelial dysfunction and progress towards the pathogenesis of DR. Previous studies have effectively proven the increased expression of adhesion protein P-selectin and ICAM in DR patient (Kamiuchi et al., 2002; Penman et al., 2015). However, this study also demonstrated a significant reduction in P-selectin after insulin suggesting that insulin could participate in preventing leukocyte adhesion thereby attenuating the progression of DR. This study could not demonstrate significance change in the ICAM-1 protein. This

could be due to difference in the endothelial cells used, the duration and the type of insulin treatment used.

This study reported that short acting insulin commonly used in the treatment of DR could control the metabolic fluxes thereby leading to improvement in oxidative stress and apoptosis. This could prevent early changes in vasodilator, adhesion and angiogenic markers such as NO, VEGFA, P-selectin involved in the angiogenesis, inflammation and neovascularization.

In conclusion, this study demonstrated that Hyperglycemia causes an increase in ROS/oxidative stress and apoptosis, while insulin promotes a significant decrease in ROS and apoptosis, eNOS mediated NO production increases with hyperglycemia but remarkably decreases with insulin treatment after 1hour, 2 hours and 4 hours, insulin could counteract the hyperglycemic effect on AKT/pI3 kinase which mediates NO production and VEGF-A, decreased adhesion molecules p-selectin involved in barrier disorder of retinal endothelial cells. Thus it could be proposed that insulin could be considered as regulators of angiogenesis.

4.2 SUMMARY OF DISCUSSION

The current study depicts the association between insulin treatment and reduction in neovascularization/angiogenesis thereby, a proposed effective treatment for improving diabetic retinopathy.

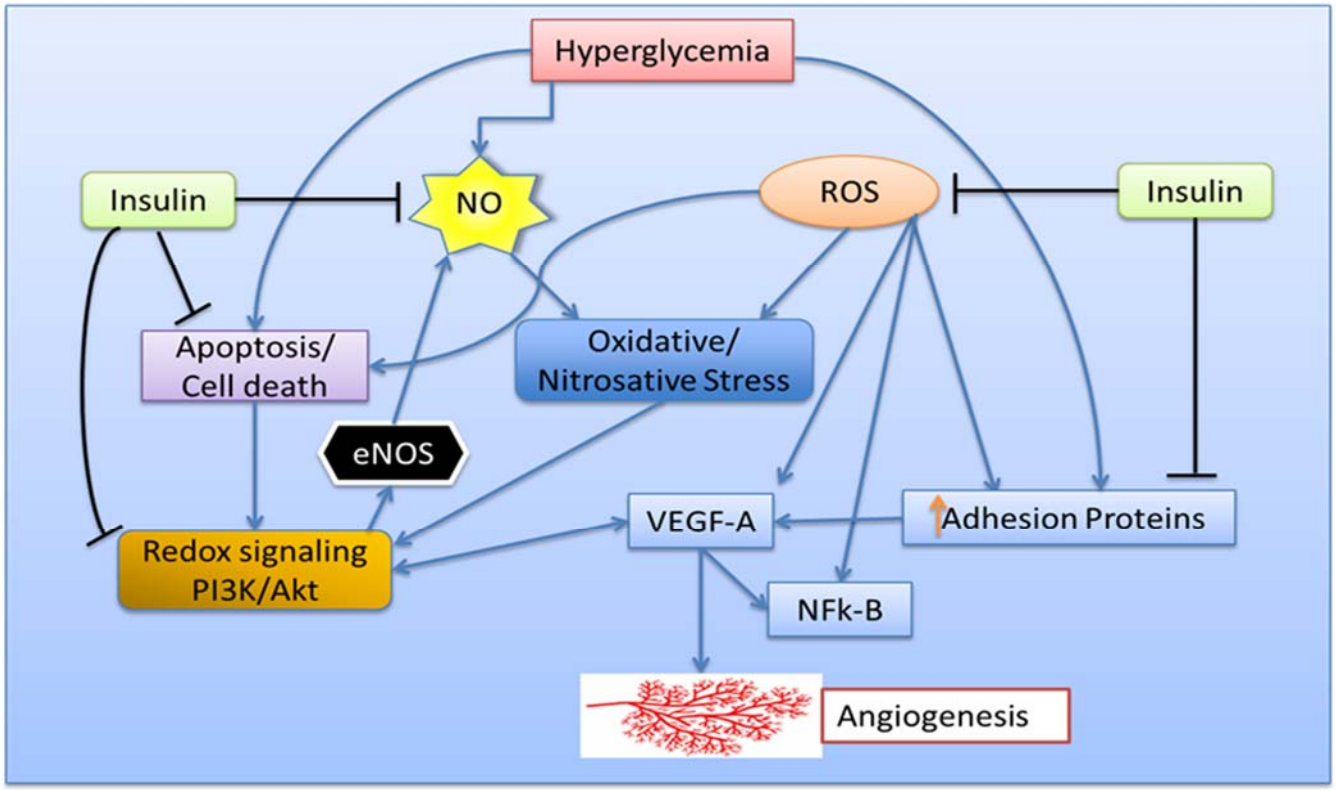

Figure4.1: Summary of discussion. Insulin as proposed negative regulator of angiogenesis.

4.3 CONCLUSION

The study shows the potent effect of short-acting insulin treatment to counteract many biomarkers and factors involved in the pathogenesis of DR and conserving microvascular function in HRECs exposed to hyperglycemia (30mM) and identifies several key factors which could be mediating insulin functioning. The beneficial effects of insulin manifested by eliciting a number of bioactive molecules in HRECs under hyperglycemia conditions. These molecules operate within complex systems and include compounds classified as NO, angiogenic factors, reactive oxygen species, adhesion proteins and various cellular proteins involved in retinal vascular functioning. Thus, the diabetic interventions using insulin as a key therapy with others may have the potential to be utilized as a readily available, safe and inexpensive to protect against microvascular complications of DR and delay its onset.

4.4 FUTURE DIRECTIONS:

Further studies are necessary to clarify the effect of insulin mediated PI3K/Akt signaling by comparison between normoglycemic and hypoglycemic condition in HRMECs. The precise mechanism of eNOS uncoupling through BH_4, its consequences and impact of upregulated ROS on eNOS needs to be explored. Assess dose dependent activity of PI3K/Akt signaling and NO production from physiological 5nM insulin to 100nM pharmacological dose to compare effect at both physiological and pharmacological doses. Confirm PI3K/Akt signaling pathway through Immunoprecipitation of phosphorylated proteins (Akt, eNOS). eNOS mediated NO production by using eNOS inhibitor L-NAME require to be confirmed. Assessment of the effect of superoxide and NO mediated peroxynitrite formation needs to be confirmed. Assess the effect of SOD (superoxide dismutates) on ROS and NO production under hyperglycemic condition. Assess PI3K/Akt pathway on VEGF-A expression and vascular permeability.

REFERENCES

Ahsan, H. (2015). Diabetic retinopathy--biomolecules and multiple pathophysiology. *Diabetes Metab Syndr, 9*(1), 51-54. doi: 10.1016/j.dsx.2014.09.011

Alderton, W. K., Cooper, C. E., & Knowles, R. G. (2001). Nitric oxide synthases: structure, function and inhibition. *Biochem J, 357*(Pt 3), 593-615.

Alves, M. e. C., Carvalheira, J. B., Módulo, C. M., & Rocha, E. M. (2008). Tear film and ocular surface changes in diabetes mellitus. Arq Bras Oftalmol, 71(6 Suppl), 96-103.

Andrew, P. J., & Mayer, B. (1999). Enzymatic function of nitric oxide synthases. *Cardiovasc Res, 43*(3), 521-531.

Anuradha, C. D., Kanno, S., & Hirano, S. (2001). Oxidative damage to mitochondria is a preliminary step to caspase-3 activation in fluoride-induced apoptosis in HL-60 cells. *Free Radic Biol Med, 31*(3), 367-373.

Bharadwaj, A. S., Appukuttan, B., Wilmarth, P. A., Pan, Y., Stempel, A. J., Chipps, T. J., . . . Smith, J. R. (2013). Role of the retinal vascular endothelial cell in ocular disease. *Prog Retin Eye Res, 32*, 102-180. doi: 10.1016/j.preteyeres.2012.08.004

Bloch-Damti, A., & Bashan, N. (2005). Proposed mechanisms for the induction of insulin resistance by oxidative stress. *Antioxid Redox Signal, 7*(11-12), 1553-1567. doi: 10.1089/ars.2005.7.1553

BRANDT, R., & KESTON, A. S. (1965). Synthesis of diacetyldichlorofluorescin: a stable reagent for fluorometric analysis. *Anal Biochem, 11*, 6-9.

Brownlee, M. (2005). The pathobiology of diabetic complications: a unifying mechanism. *Diabetes, 54*(6), 1615-1625.

Caballero, A. E., Arora, S., Saouaf, R., Lim, S. C., Smakowski, P., Park, J. Y., . . . Veves, A. (1999). Microvascular and macrovascular reactivity is reduced in subjects at risk for type 2 diabetes. *Diabetes, 48*(9), 1856-1862.

Chakravarthy, U., Hayes, R. G., Stitt, A. W., McAuley, E., & Archer, D. B. (1998). Constitutive nitric oxide synthase expression in retinal vascular endothelial cells is suppressed by high glucose and advanced glycation end products. *Diabetes, 47*(6), 945-952.

Chen, Z., Liu, G., Xiao, Y., & Lu, P. (2014). Adrenomedullin22-52 suppresses high-glucose-induced migration, proliferation, and tube formation of human retinal endothelial cells. *Mol Vis, 20*, 259-269.

Cheung, N., Mitchell, P., & Wong, T. Y. (2010). Diabetic retinopathy. *Lancet, 376*(9735), 124-136. doi: 10.1016/S0140-6736(09)62124-3

Cines, D. B., Pollak, E. S., Buck, C. A., Loscalzo, J., Zimmerman, G. A., McEver, R. P., . . . Stern, D. M. (1998). Endothelial cells in physiology and in the pathophysiology of vascular disorders. *Blood, 91*(10), 3527-3561.

Cosentino, F., Hishikawa, K., Katusic, Z. S., & Lüscher, T. F. (1997). High glucose increases nitric oxide synthase expression and superoxide anion generation in human aortic endothelial cells. *Circulation, 96*(1), 25-28.

Cosentino, F., & Lüscher, T. F. (1998). Tetrahydrobiopterin and endothelial function. *Eur Heart J, 19 Suppl G*, G3-8.

Dimmeler, S., Fleming, I., Fisslthaler, B., Hermann, C., Busse, R., & Zeiher, A. M. (1999). Activation of nitric oxide synthase in endothelial cells by Akt-dependent phosphorylation. *Nature, 399*(6736), 601-605. doi: 10.1038/21224

Dröge, W. (2002). Free radicals in the physiological control of cell function. *Physiol Rev, 82*(1), 47-95. doi: 10.1152/physrev.00018.2001

Du, X., Stocklauser-Färber, K., & Rösen, P. (1999). Generation of reactive oxygen intermediates, activation of NF-kappaB, and induction of apoptosis in human endothelial cells by glucose: role of nitric oxide synthase? *Free Radic Biol Med, 27*(7-8), 752-763.

Du, Y., Miller, C. M., & Kern, T. S. (2003). Hyperglycemia increases mitochondrial superoxide in retina and retinal cells. *Free Radic Biol Med, 35*(11), 1491-1499.

Favero, G., Paganelli, C., Buffoli, B., Rodella, L. F., & Rezzani, R. (2014). Endothelium and its alterations in cardiovascular diseases: life style intervention. *Biomed Res Int, 2014*, 801896. doi: 10.1155/2014/801896

Förstermann, U. (2008). Oxidative stress in vascular disease: causes, defense mechanisms and potential therapies. *Nat Clin Pract Cardiovasc Med, 5*(6), 338-349. doi: 10.1038/ncpcardio1211

Förstermann, U. (2010). Nitric oxide and oxidative stress in vascular disease. *Pflugers Arch, 459*(6), 923-939. doi: 10.1007/s00424-010-0808-2

Gao, R., Zhu, B. H., Tang, S. B., Wang, J. F., & Ren, J. (2008). Scutellarein inhibits hypoxia- and moderately-high glucose-induced proliferation and VEGF expression in human retinal endothelial cells. *Acta Pharmacol Sin, 29*(6), 707-712. doi: 10.1111/j.1745-7254.2008.00797.x

Gewaltig, M. T., & Kojda, G. (2002). Vasoprotection by nitric oxide: mechanisms and therapeutic potential. *Cardiovasc Res, 55*(2), 250-260.

Giacco, F., & Brownlee, M. (2010). Oxidative stress and diabetic complications. *Circ Res, 107*(9), 1058-1070. doi: 10.1161/CIRCRESAHA.110.223545

Griendling, K. K., Sorescu, D., & Ushio-Fukai, M. (2000). NAD(P)H oxidase: role in cardiovascular biology and disease. *Circ Res, 86*(5), 494-501.

Griscavage, J. M., Wilk, S., & Ignarro, L. J. (1996). Inhibitors of the proteasome pathway interfere with induction of nitric oxide synthase in macrophages by blocking activation of transcription factor NF-kappa B. *Proc Natl Acad Sci U S A, 93*(8), 3308-3312.

Groop, P. H., Forsblom, C., & Thomas, M. C. (2005). Mechanisms of disease: Pathway-selective insulin resistance and microvascular complications of diabetes. *Nat Clin Pract Endocrinol Metab, 1*(2), 100-110. doi: 10.1038/ncpendmet0046

Kalani, M. (2008). The importance of endothelin-1 for microvascular dysfunction in diabetes. *Vasc Health Risk Manag, 4*(5), 1061-1068.

Kamiuchi, K., Hasegawa, G., Obayashi, H., Kitamura, A., Ishii, M., Yano, M., . . . Nakamura, N. (2002). Intercellular adhesion molecule-1 (ICAM-1) polymorphism is associated with diabetic retinopathy in Type 2 diabetes mellitus. *Diabet Med, 19*(5), 371-376.

Kearney, M. T., Duncan, E. R., Kahn, M., & Wheatcroft, S. B. (2008). Insulin resistance and endothelial cell dysfunction: studies in mammalian models. *Exp Physiol, 93*(1), 158-163. doi: 10.1113/expphysiol.2007.039172

Khalfaoui, T., Lizard, G., & Ouertani-Meddeb, A. (2008). Adhesion molecules (ICAM-1 and VCAM-1) and diabetic retinopathy in type 2 diabetes. *J Mol Histol, 39*(2), 243-249. doi: 10.1007/s10735-007-9159-5

Kim, F., Gallis, B., & Corson, M. A. (2001). TNF-alpha inhibits flow and insulin signaling leading to NO production in aortic endothelial cells. *Am J Physiol Cell Physiol, 280*(5), C1057-1065.

Kojima, H., Sakurai, K., Kikuchi, K., Kawahara, S., Kirino, Y., Nagoshi, H., . . . Nagano, T. (1998). Development of a fluorescent indicator for nitric oxide based on the fluorescein chromophore. *Chem Pharm Bull (Tokyo), 46*(2), 373-375.

Kolka, C. M., & Bergman, R. N. (2013). The endothelium in diabetes: its role in insulin access and diabetic complications. *Rev Endocr Metab Disord, 14*(1), 13-19. doi: 10.1007/s11154-012-9233-5

Kowluru, R. A., Abbas, S. N., & Odenbach, S. (2004). Reversal of hyperglycemia and diabetic nephropathy: effect of reinstitution of good metabolic control on oxidative stress in the kidney of diabetic rats. *J Diabetes Complications, 18*(5), 282-288. doi: 10.1016/j.jdiacomp.2004.03.002

Kowluru, R. A., & Chan, P. S. (2007). Oxidative stress and diabetic retinopathy. *Exp Diabetes Res, 2007*, 43603. doi: 10.1155/2007/43603

Kowluru, R. A., & Koppolu, P. (2002). Diabetes-induced activation of caspase-3 in retina: effect of antioxidant therapy. *Free Radic Res, 36*(9), 993-999.

Kowluru, R. A., Koppolu, P., Chakrabarti, S., & Chen, S. (2003). Diabetes-induced activation of nuclear transcriptional factor in the retina, and its inhibition by antioxidants. *Free Radic Res, 37*(11), 1169-1180.

Kowluru, R. A., Tang, J., & Kern, T. S. (2001). Abnormalities of retinal metabolism in diabetes and experimental galactosemia. VII. Effect of long-term administration of antioxidants on the development of retinopathy. *Diabetes, 50*(8), 1938-1942.

Kumari, S., Panda, S., Mangaraj, M., Mandal, M. K., & Mahapatra, P. C. (2008). Plasma MDA and antioxidant vitamins in diabetic retinopathy. *Indian J Clin Biochem, 23*(2), 158-162. doi: 10.1007/s12291-008-0035-1

Ley, K., Bullard, D. C., Arbonés, M. L., Bosse, R., Vestweber, D., Tedder, T. F., & Beaudet, A. L. (1995). Sequential contribution of L- and P-selectin to leukocyte rolling in vivo. *J Exp Med, 181*(2), 669-675.

Life Technologies. (2015, Aprilr Thrusday). *XCell II™ Blot Module - Life Technologies*. Retrieved from https://tools.lifetechnologies.com/content/sfs/manuals/blotmod_pro.pdf

Liu, Y., Burdon, K. P., Langefeld, C. D., Beck, S. R., Wagenknecht, L. E., Rich, S. S., . . . Freedman, B. I. (2005). P-selectin gene haplotype associations with albuminuria in the Diabetes Heart Study. *Kidney Int, 68*(2), 741-746. doi: 10.1111/j.1523-1755.2005.00452.x

Madsen-Bouterse, S. A., & Kowluru, R. A. (2008). Oxidative stress and diabetic retinopathy: pathophysiological mechanisms and treatment perspectives. *Rev Endocr Metab Disord, 9*(4), 315-327. doi: 10.1007/s11154-008-9090-4

Matsumoto, K., Sera, Y., Ueki, Y., Inukai, G., Niiro, E., & Miyake, S. (2002). Comparison of serum concentrations of soluble adhesion molecules in diabetic microangiopathy and macroangiopathy. *Diabet Med, 19*(10), 822-826.

Mayer, B., & Hemmens, B. (1997). Biosynthesis and action of nitric oxide in mammalian cells. *Trends Biochem Sci, 22*(12), 477-481.

McLeod, D. S., Lefer, D. J., Merges, C., & Lutty, G. A. (1995). Enhanced expression of intracellular adhesion molecule-1 and P-selectin in the diabetic human retina and choroid. *Am J Pathol, 147*(3), 642-653.

Melissa DeAnn Shelton, T. S. K. a. J. J. M. (2007). Activation of NFkB and Increased Pro-Inflammatory ICAM-1 in Retinal Glial (Müller) Cells in High Glucose, a Model of Diabetic Retinopathy, is Mediated via Upregulation of Glutaredoxin. *The FASEB Journal*, 21:816.817.

Mitamura, Y., Harada, T., Harada, C., Ohtsuka, K., Kotake, S., Ohno, S., . . . Wada, K. (2003). NF-kappaB in epiretinal membranes after human diabetic retinopathy. *Diabetologia, 46*(5), 699-703. doi: 10.1007/s00125-003-1084-x

Mizutani, M., Kern, T. S., & Lorenzi, M. (1996). Accelerated death of retinal microvascular cells in human and experimental diabetic retinopathy. *J Clin Invest, 97*(12), 2883-2890. doi: 10.1172/JCI118746

Montagnani, M., Chen, H., Barr, V. A., & Quon, M. J. (2001). Insulin-stimulated activation of eNOS is independent of Ca2+ but requires phosphorylation by Akt at Ser(1179). *J Biol Chem, 276*(32), 30392-30398. doi: 10.1074/jbc.M103702200

Mortensen, A., & Lykkesfeldt, J. (2014). Does vitamin C enhance nitric oxide bioavailability in a tetrahydrobiopterin-dependent manner? In vitro, in vivo and clinical studies. *Nitric Oxide, 36*, 51-57. doi: 10.1016/j.niox.2013.12.001

Nakagawa, T., Sato, W., Sautin, Y. Y., Glushakova, O., Croker, B., Atkinson, M. A., . . . Johnson, R. J. (2006). Uncoupling of vascular endothelial growth factor with nitric oxide as a mechanism for diabetic vasculopathy. *J Am Soc Nephrol, 17*(3), 736-745. doi: 10.1681/ASN.2005070759

Ola, M. S., Nawaz, M. I., Siddiquei, M. M., Al-Amro, S., & Abu El-Asrar, A. M. (2012). Recent advances in understanding the biochemical and molecular mechanism of diabetic retinopathy. *J Diabetes Complications, 26*(1), 56-64. doi: 10.1016/j.jdiacomp.2011.11.004

Pandey, G., Makhija, E., George, N., Chakravarti, B., Godbole, M. M., Ecelbarger, C. M., & Tiwari, S. (2015). Insulin regulates nitric oxide production in the kidney collecting duct cells. *J Biol Chem, 290*(9), 5582-5591. doi: 10.1074/jbc.M114.592741

Patel, S., & Santani, D. (2009). Role of NF-kappa B in the pathogenesis of diabetes and its associated complications. *Pharmacol Rep, 61*(4), 595-603.

Penman, A., Hoadley, S., Wilson, J. G., Taylor, H. A., Chen, C. J., & Sobrin, L. (2015). P-selectin Plasma Levels and Genetic Variant Associated With Diabetic Retinopathy in African Americans. *Am J Ophthalmol*. doi: 10.1016/j.ajo.2015.03.008

Phaneuf, S., & Leeuwenburgh, C. (2002). Cytochrome c release from mitochondria in the aging heart: a possible mechanism for apoptosis with age. *Am J Physiol Regul Integr Comp Physiol, 282*(2), R423-430. doi: 10.1152/ajpregu.00296.2001

Pries, A. R., & Kuebler, W. M. (2006). Normal endothelium. *Handb Exp Pharmacol*(176 Pt 1), 1-40.

Rangasamy, S., McGuire, P. G., & Das, A. (2012). Diabetic retinopathy and inflammation: novel therapeutic targets. *Middle East Afr J Ophthalmol, 19*(1), 52-59. doi: 10.4103/0974-9233.92116

Reiter, C. E., & Gardner, T. W. (2003). Functions of insulin and insulin receptor signaling in retina: possible implications for diabetic retinopathy. *Prog Retin Eye Res, 22*(4), 545-562.

Reiter, C. E., Wu, X., Sandirasegarane, L., Nakamura, M., Gilbert, K. A., Singh, R. S., . . . Gardner, T. W. (2006). Diabetes reduces basal retinal insulin receptor signaling: reversal with systemic and local insulin. *Diabetes, 55*(4), 1148-1156.

Resta, T. C., Gonzales, R. J., Dail, W. G., Sanders, T. C., & Walker, B. R. (1997). Selective upregulation of arterial endothelial nitric oxide synthase in pulmonary hypertension. *Am J Physiol, 272*(2 Pt 2), H806-813.

Romeo, G., Liu, W. H., Asnaghi, V., Kern, T. S., & Lorenzi, M. (2002). Activation of nuclear factor-kappaB induced by diabetes and high glucose regulates a proapoptotic program in retinal pericytes. *Diabetes, 51*(7), 2241-2248.

Salt, I. P., Morrow, V. A., Brandie, F. M., Connell, J. M., & Petrie, J. R. (2003). High glucose inhibits insulin-stimulated nitric oxide production without reducing endothelial nitric-oxide synthase Ser1177 phosphorylation in human aortic endothelial cells. *J Biol Chem, 278*(21), 18791-18797. doi: 10.1074/jbc.M210618200

Scherrer, U., Randin, D., Vollenweider, P., Vollenweider, L., & Nicod, P. (1994). Nitric oxide release accounts for insulin's vascular effects in humans. *J Clin Invest, 94*(6), 2511-2515. doi: 10.1172/JCI117621

Schmetterer, L., & Polak, K. (2001). Role of nitric oxide in the control of ocular blood flow. *Prog Retin Eye Res, 20*(6), 823-847.

Shankar, R. R., Wu, Y., Shen, H. Q., Zhu, J. S., & Baron, A. D. (2000). Mice with gene disruption of both endothelial and neuronal nitric oxide synthase exhibit insulin resistance. *Diabetes, 49*(5), 684-687.

Sobrevia, L., Nadal, A., Yudilevich, D. L., & Mann, G. E. (1996). Activation of L-arginine transport (system y+) and nitric oxide synthase by elevated glucose and insulin in human endothelial cells. *J Physiol, 490 (Pt 3)*, 775-781.

Sobrin, L., Green, T., Sim, X., Jensen, R. A., Tai, E. S., Tay, W. T., . . . 2, W. T. C. C. C. (2011). Candidate gene association study for diabetic retinopathy in persons with type 2 diabetes: the Candidate gene Association Resource (CARe). *Invest Ophthalmol Vis Sci, 52*(10), 7593-7602. doi: 10.1167/iovs.11-7510

Sánchez, A., Martínez, P., Muñoz, M., Benedito, S., García-Sacristán, A., Hernández, M., & Prieto, D. (2014). Endothelin-1 contributes to endothelial dysfunction and enhanced vasoconstriction through augmented superoxide production in penile arteries from insulin-resistant obese rats: role of ET(A) and ET(B) receptors. *Br J Pharmacol, 171*(24), 5682-5695. doi: 10.1111/bph.12870

Tedder, T. F., Steeber, D. A., Chen, A., & Engel, P. (1995). The selectins: vascular adhesion molecules. *FASEB J, 9*(10), 866-873.

Toda, N., & Nakanishi-Toda, M. (2007). Nitric oxide: ocular blood flow, glaucoma, and diabetic retinopathy. *Prog Retin Eye Res, 26*(3), 205-238. doi: 10.1016/j.preteyeres.2007.01.004

Vásquez-Vivar, J., Kalyanaraman, B., Martásek, P., Hogg, N., Masters, B. S., Karoui, H., . . . Pritchard, K. A. (1998). Superoxide generation by endothelial nitric oxide synthase: the influence of cofactors. *Proc Natl Acad Sci U S A, 95*(16), 9220-9225.

Wheatcroft, S. B., Kearney, M. T., Shah, A. M., Grieve, D. J., Williams, I. L., Miell, J. P., & Crossey, P. A. (2003). Vascular endothelial function and blood pressure homeostasis in mice overexpressing IGF binding protein-1. *Diabetes, 52*(8), 2075-2082.

Wheatcroft, S. B., Williams, I. L., Shah, A. M., & Kearney, M. T. (2003). Pathophysiological implications of insulin resistance on vascular endothelial function. *Diabet Med, 20*(4), 255-268.

World Health Organization. (2015, January Saturday). *Medica Center/ Fact sheet*. Retrieved from http://www.who.int/mediacentre/factsheets/fs312/en/

Wu, H., Xia, X., Jiang, C., Wu, J., Zhang, S., Zheng, Z., . . . Xu, X. (2010). High glucose attenuates insulin-induced VEGF expression in bovine retinal microvascular endothelial cells. *Eye (Lond), 24*(1), 145-151. doi: 10.1038/eye.2009.157

Yamagishi, S., & Matsui, T. (2011). Advanced glycation end products (AGEs), oxidative stress and diabetic retinopathy. *Curr Pharm Biotechnol, 12*(3), 362-368.

Yoshizumi, M., Perrella, M. A., Burnett, J. C., & Lee, M. E. (1993). Tumor necrosis factor downregulates an endothelial nitric oxide synthase mRNA by shortening its half-life. *Circ Res, 73*(1), 205-209.

Yu, D. Y., Yu, P. K., Cringle, S. J., Kang, M. H., & Su, E. N. (2014). Functional and morphological characteristics of the retinal and choroidal vasculature. *Prog Retin Eye Res, 40*, 53-93. doi: 10.1016/j.preteyeres.2014.02.001

Yu, P., Yu, D. M., Qi, J. C., Wang, J., Zhang, Q. M., Zhang, J. Y., . . . Li, M. Z. (2006). [High D-glucose alters PI3K and Akt signaling and leads to endothelial cell migration, proliferation and angiogenesis dysfunction]. *Zhonghua Yi Xue Za Zhi, 86*(48), 3425-3430.

Zeng, G., & Quon, M. J. (1996). Insulin-stimulated production of nitric oxide is inhibited by wortmannin. Direct measurement in vascular endothelial cells. *J Clin Invest, 98*(4), 894-898. doi: 10.1172/JCI118871

Zou, M. H., Shi, C., & Cohen, R. A. (2002). Oxidation of the zinc-thiolate complex and uncoupling of endothelial nitric oxide synthase by peroxynitrite. *J Clin Invest, 109*(6), 817-826. doi: 10.1172/JCI14442

APPENDIX

جامعة قطر
QATAR UNIVERSITY

Qatar University
Institutional Bio-safety Committee

To: Dr. Nasser Rizk
Department of Health Sciences
College of Arts and Science

2nd Sept, 2014

Dear Dr. Rizk

Subject: Research grant: QUST-CAS-SPR-13/14-20

Ref: Project titled "Association between insulin resistance and nitric oxide in retinal vascular endothelial cells in vitro"

We would like to inform you that your application along with supporting documents provided for the above proposal have been reviewed by QU-IBC, and having met all the requirements, has been granted approval for a period of one year and renewable for each year thereafter, should be sought and approved by QU-IBC period to continue.

Please note that QU-IBC approval is contingent upon your adherence to the following QU-IBC Guidelines:

- Ensuring compliance with QU Safety Plans and applicable national and international regulations.
- Ensuring experiments that require prior IBC approval are not conducted until IBC approval is obtained and making initial determination of containment levels required for experiments.
- Notifying the IBC of any changes to other hazardous material experiments previously approved by the IBC.
- Reporting any significant problems, violations of QU Safety Plans and applicable regulations/guidelines, or any significant research-related accidents and illnesses to the QU-IBC. Also, ensuring personnel receive appropriate orientation and specific training for the safe performance of the work.

Your research approval No. is: **QU-IBC 2/14-15**. Please refer to this approval number in all your future correspondence pertaining to this research.

Best wishes.

Dr. Marawan Abu-Madi PhD, MLS(ASCP)cm
Chairperson, QU-IBC
Department of Health Sciences
College of Arts & Sciences
Qatar University
Tel: +974 4403 4791
abumadi@qu.edu.qa

جامعة قطر
Institutional Bio-safety Committee
(IBC)
Office of Academic Research